PROCEEDINGS OF THE 24TH INTERNATIONAL APPLIED GEOCHEMISTRY SYMPOSIUM

FREDERICTON, NEW BRUNSWICK, CANADA

JUNE 1ST-4TH, 2009

EDITED BY

DAVID R. LENTZ, KATHLEEN G. THORNE, & KRISTY-LEE BEAL

VOLUME I

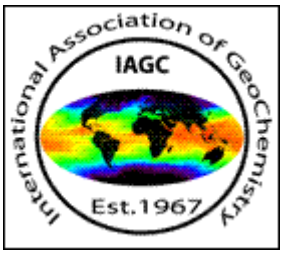

ISBN 978-1-55131-136-4

PROCEEDINGS OF THE 24TH INTERNATIONAL APPLIED GEOCHEMISTRY SYMPOSIUM

FREDERICTON, NEW BRUNSWICK
CANADA
JUNE 1ST-4TH, 2009

EDITED BY

DAVID R. LENTZ
KATHLEEN G. THORNE
KRISTY-LEE BEAL

VOLUME I

TECHNICAL EDITORS

(Listed in alphabetical order)

Mark Arundell
U. Aswathanarayana
Roger Beckie
Chris Benn
Robert Bowell
Charles Butt
Bill Coker
Hugh deSouza
Sara Fortner
David Gladwell
Wayne Goodfellow
Eric Grunsky
William Gunter
Gwendy Hall
Jacob Hanley
Russell Harmon
David Heberlein
Brian Hitchon
Andrew Kerr
Dan Kontak
Kurt Kyser
David Lentz
Ray Lett
Matthew Leybourne
Steven McCutcheon
Beth McClenaghan
Nancy McMillan
Paul Morris
Lee Ann Munk
Dogan Paktunc
Roger Paulen
Ernie Perkins
David Quirt
Andy Rencz
David Smith
Cliff Stanley
Gerry Stanley
Nick Susak
Bruce Taylor
Ed Van Hees
James Walker
Lawrence Winter

USING ISOTOPE GEOCHEMISTRY TO EXPLORE FOR RESOURCES

EDITED BY:

ED VAN HEES
KURT KYSER
BRUCE TAYLOR

Isotopic studies and comparison of marbles in the Sambagawa metamorphic belt, central Shikoku, Japan and marbles from the Kumdy-Kol area of Kokchetav Massif, North Kazakhstan

Zaure Bekmukhametova[1]

[1]*Kazakh-British Technical University, 05000, Tolebi 59, Almaty KAZAKHSTAN (e-mail: zaureb31@yahoo.com)*

ABSTRACT: Carbon and oxygen isotope studies were carried out on marbles occurring in epidote amphibolite masses from the Tonaru and Iratsu areas of the Sambagawa metamorphic belt, Japan and the Kumdy-Kol area of the Kokchetav Massif, Kazakhstan to compare them and to elucidate their origin. Based on the results of carbon and oxygen isotope analyses, marbles from the Tonaru and Iratsu areas were probably precipitated from sea water as their $\delta^{13}C$ values corresponds to those of marine carbonates. In contrast, $\delta^{13}C$ values of diamond-bearing dolomitic marbles from the Kumdy-Kol area corresponds to mantle carbon and their origin can be interpreted as having been derived from magmatic or deep-seated carbonates.

KEYWORDS: *carbon, oxygen, isotopic, analysis, marble*

INTRODUCTION

Marbles occur in many regional and contact metamorphic terrains in the world and isotopic studies of marbles have been carried out and report by many authors. Carbon isotope studies of marbles can be useful, in many cases, to reveal the origin of carbonates because differences in carbon isotope ratios of marbles can reflect different origins.

Carbon and oxygen isotope analyses were carried out on marbles occurring in the epidote amphibolite masses from the Iratsu and Tonaru areas of the Sanbagawa metamorphic belt, central Shikoku, Japan and on diamond-bearing dolomitic marbles from the Kumdy-Kol site of the Kokchetav Massif, to compare them and to elucidate their origin.

MARBLES FROM THE SAMBAGAWA METAMORPIC BELT, JAPAN

The Sambagawa metamorphic belt of central Shikoku is part of the intermediate high-pressure metamorphic belt in Japan. Marbles examined in this study were collected from Iratsu (samples Ta-01~Ta-14) and Tonaru (samples Ta-15~Ta16), as well as and epidote amphibolites masses from each area representing metamorphosed layered gabbro complexes, which were subjected to the Sambagawa metamorphism of epidote amphibolite facies (Banno *et.al*. 1976; Takasu & Makino 1980). The marbles occur in lenticular form, about 1m maximum in width, intercalated concordantly or subconcordantly in the host epidote amphibolite, and composed mainly of calcite, diopside, hornblende and epidote with subordinate amounts of chlorite, muscovite, albite, quartz, and sphene.

According to Wada *et al*. (1984), the marbles from the Sambagawa metamorphic belt are isotopically classified into two groups. The first group comprises marbles in epidote amphibolite masses and the second includes marbles from the crystalline schists and from the marginal parts of the epidote amphibolite masses. These marbles were collected from the Hadeba, Fijiwara and Matsuno areas. Hadeba and Fujiwara areas belong to the high-grade portion of the garnet zone or the transitional part between the garnet and albite-biotite zones. In both areas, the marbles occur in lenticular form, about 3-40 cm in width. These marbles are composed mainly of calcite, graphite, diopside, tremolite and zoisite with subordinate amounts of chlorite,

muscovite, albite, quartz and sphene.

MARBLES FROM THE KOKCHETAV MASSIF, KAZAKHSTAN

The Kokchetav Massif of northern Kazakhstan is a very large, fault-bounded metamorphic complex of Late Proterozoic-Paleozoic protolith age, surrounded by the Caledonian rocks of the Ural-Mongolian fold belt. The Kokchetav UHP and HP belt runs NW-SE extending at least 150 km long and 17 km wide. This massif has attracted much interest since the discovery of metamorphic diamonds. It is the first locality where microdiamonds were found within metamorphic rocks derived from crustal material.

Diamond-bearing rocks within the Zerendin series include garnet-biotite gneiss, garnet-kyanite-muscovite-quartz schist, marble and eclogite. These kinds of rocks can be traced for a distance of about 100 km.

Marbles examined in this study were collected from the Kumdy-Kol area of the Kokchetav Massif I (samples Ku 1~Ku-3). Ogasawara *et al.* (2000) divided metacarbonate rocks from the Kumdy-Kol area of Kokchetav Massif into diamond-bearing dolomite marbles and diamond-free dolomitic marbles. Diamond-bearing dolomitic marble has been described as pyroxene-carbonate-garnet rock (Sobolev & Shatsky 1990) and as diamondiferous carbonate rock (Vavilov & Shatsky 1993). These two types of carbonate rocks were collected from an outcrop and a waste deposit at the Kumdy-Kol area. Ogasawara *et al*. (2000) also divided metacarbonate rocks from Kumdy-Kol area into diamond-bearing dolomite marbles and diamond-free dolomitic marbles. The differences in mineral assemblages in both types of marbles are explained by the local heterogeneity of the fluid compositions (Sobolev & Shatsky 1990).

Diamond-bearing Marbles:

Diamond-bearing marbles show granoblastic texture and this type of carbonate contains abundant microdiamond with or without graphite. The mineral assemblage of diamond-bearing marble is mainly garnet and clinopyroxene with interstitial calcite and phlogopite. Accessory minerals include rutile and titanite, chlorite, quartz, K-feldspar and kyanite. The diamonds are cubo-octahedral, 12 μm in size on average and occur in zircons. They also occur in garnet with euhedral graphite (c.50 μm across) as inclusions. Graphite occurs on the surface of diamond crystals, and as secondary crystals (≤ 300 μm) in intergranular areas.

Diamond-free Marbles

These marbles show equigranular granoblastic texture, and according to Ogasawara *et al*. (2000), are characterized by the absence of graphite and diamond. They consist mainly of Mg-calcite + dolomite +forsterite + diopside + Ti-clinohumite. Garnet is replaced by symplectite of diopside, spinel and Mg-calcite, plus minor amounts of pyrrhotite, pyrite and chalcopyrite.

Two types of marbles occur as small, lenticular, banded or vein-like bodies within garnet-pyroxene and tremolite-chlorite-bearing quartzites, plagioclase gneisses, garnet-biotite and biotite gneisses of the Zerendinsk rocks series. Their field relation are not well known, but the features of these rocks suggest that two rock types probably were subjected to UHP metamorphic rocks at the same P-T conditions (Sobolev & Shatsky 1990, Ogasawara *et al.* 2000).

SAMPLES AND EXPERIMENTS

Carbon and oxygen isotope compositions of sixteen marbles from epidote amphibolites of the Sambagawa metamorphic belt and of three diamond-bearing marbles from the Kumdy-Kol area of Kokchetav Massif were measured. Powdered calcite from the marbles was decomposed by 100 percent phosphoric acid at 60^{o}C to obtain carbon dioxide gas for isotopic analyses. Isotopic measurements were carried out using a triple-collector mass spectrometer (Finnigan MAT Delta E). All data are given in terms of a conventional expression in

Table 1. Isotopic composition of calcite in marbles collected from epidote amphibolite masses of the Sambagawa metamorphic belt, central Shikoku.

Sample	$\delta^{13}C$	$\delta^{18}O_{PDB}$	$\delta^{18}O_{SMOW}$
Iratsu area			
Ta-01	1.2	-15.2	15.2
Ta-02	1.3	-15.6	14.9
Ta-03	0.6	-14.5	15.9
Ta-04	3.6	-16.2	14.2
Ta-05	2.2	-12.6	17.9
Ta-06	3.4	-12.2	18.3
Ta-07	1.0	-15.0	15.5
Ta-08	-0.2	-16.6	13.8
Ta-09	1.8	-13.9	16.6
Ta-10	1.3	-17.9	12.4
Ta-11	0.0	-12.7	17.8
Ta-12	1.6	-16.4	14.0
Ta-13	-0.9	-16.4	14.0
Ta-14	0.6	-14.2	16.3
Tonaru area			
Ta-15	0.3	-16.0	14.5
Ta-16	-1.8	-18.1	12.3

per mil unit relative to PDB for $^{13}C/^{12}C$ and SMOW for $^{18}O/^{16}O$ ratios $\delta(‰)$ = (R(sample)/R(standard) -1) x 1,000, where R is the ratio in a sample and the standard.

The standard deviation of several independent analyses for the same material is about 0.05 and 0.1 ‰ for $\delta^{13}C$ and $\delta^{18}O$, respectively.

Carbon and oxygen isotope compositions of calcite in marbles collected from the Sambagawa metamorphic belt are given in Table 1. For calcites from 16 selected marbles from Iratsu and Tonaru areas of the Sambagawa metamorphic belt, we obtained $\boldsymbol{\delta^{13}C_{PDB}}$ values that range from –1.8 to +3.6 ‰ and $\boldsymbol{\delta^{18}O_{SMOW}}$ values of +12.3 to +17.9 ‰.

Carbon and oxygen isotope compositions of calcite in marbles collected from the Komdy-Kol area of the Kokchetav Massif are given in Table 2. $\boldsymbol{\delta^{13}C_{PDB}}$ values of calcites of diamond-bearing marbles from the Kokchetav Massif are distinctly lower than those from the Iratsu and Tonaru areas, and fall in the range of mafic and ultramafic rocks between –5.2 to –8.4 ‰ with $\boldsymbol{\delta^{18}O_{SMOW}}$ values of +13.7 to +17.2 ‰.

Table 2. Isotopic composition of calcite in marbles collected from the Komdy-Kol area of Kokchetav Massif

Sample	$\delta^{13}C_{PDB}$	$\delta^{18}O_{PDB}$	$\delta^{18}O_{SMOW}$
Ku-1	-5.2	-13.2	17.2
Ku-2	-8.4	-13.7	16.8
Ku-3	-6.4	-16.7	13.7

CONCLUSIONS

Based on our analyses, we conclude that the marbles from the Sambagawa metamorphic belt and those from the Kokchetav Massif have different origins.

Carbon and oxygen isotopic analyses show that marbles from the Iratsu and Tonaru areas in the Sambagawa metamorphic belt have $\boldsymbol{\delta^{13}C_{PDB}}$ values close to zero, similar to most marine carbonates. These data suggest that these marbles have precipitated from sea water.

Taking into account the negative $\boldsymbol{\delta^{13}C_{PDB}}$ values of marbles from the Komdy-Kol area, we propose a different origin from the marbles in the Sambagawa metamorphic belt. The origin of the Komdy-Kol marbles is interpreted as rocks derived from magmatic or deep-seated carbonates. The difference in mineral assemblage in diamond-bearing and diamond-free marbles from the same outcrop and deposit at the Kumdy-Kol area in the Kokchetav Massif is explained by local heterogeneity of the fluid composition and by the differences in CO_2 condition.

ACKNOWLEDGEMENTS

I wish to express many thanks to professor Akira Takasu of Shimane University, Japan, who was my supervisor during my stay in Japan for his support, teaching and useful suggestions. I also wish to thank professor Seto for his help to carry out isotopic analyses of my samples and Dr. Sampei for his helpful comments.

REFERENCES

BANNO, S. & YOKOYAMA, K., IWATA, O., &

TERASHIMA, S. 1976. Genesis of epidote amphibolite masses in the Sanbagawa metamorphic belt of central Shikoku. *Geological Society of Japan*, **82**, 199-210.

OGASAWARA, Y. & OHTA, M. *et al.* 2000. Diamond-bearing and diamond-free metacarbonate rocks from Kumdy-Kol in the Kokchetav Massif, northern Kazakhstan. *The Island Arc*, **9**, 400-416.

SHATSKY, V.S., SOBOLEV, N.V., & VAVILOV, M.A. 1995. *Diamond-bearing metamorphic rocks of the Kokchetav Massif (northern Kazakhstan). Ultrahigh-Pressure Metamorphism*. Cambridge University Press, Cambridge, 425-455.

SOBOLEV, N.V. & SHATSKY, V.S. 1990. Diamond inclusions in garnets from metamorphic rocks. *Nature*, **343**, 742-746.

TAKASU, A. & MAKINO, K. 1980. Stratigraphy and geologic structure of the Sambagawa metamorphic belt in the Bessi district, Shikoku, Japan-reexamination of the recumbent fold structures. *Chikyu Kagaku*, (Earth Science), **34**, 16-26.

WADA, H. & ENAMI, M. 1984. Isotopic composition of marbles in the Sanbagawa metamorphic terrain, central Shikoku. *Japan Geochemical Journal*, **18**, 61-73.

Cu Isotope Study of the Silver Bell Porphyry Cu Mine

Molly Dendas[1], Ryan Mathur[1], & Spencer Titley[2]
[1]*Juniata College, 1700 Moore St, Huntingdon, PA USA*
(email: dendamm06@juniata.edu)
[2]*University of Arizona, Gould-Simpson Building #77, 1040 E 4th St., Tucson, AZ, 85721 USA*

ABSTRACT: Silver Bell is a typical porphyry Cu deposit of the American southwest that has experienced intense weathering and remobilization of Cu during supergene processes. Cu isotope analyses of hematite, goethite, and jarosite from the leached cap, and chalcopyrite, cuprite, and chalcocite from the enrichment blanket at the Silver Bell Mine in Arizona reveal correlations between isotopic compositions and Cu concentrations of the minerals. Leach caps contain significantly lower amounts of Cu than enrichment blankets, and lighter Cu isotopic compositions, averaging -6.9‰. In contrast, the enrichment blankets contain heavier isotopic compositions averaging 5.4‰, therefore indicating that a rough mass balance exists between the two isotopic reservoirs. Isotopic fractionation of Cu is substantial during the leaching process, and could be used as an exploration tool.

KEYWORDS: *Cu isotopes, leaching process, Cu fractionation, supergene*

INTRODUCTION

The goal of this project is to find a geochemical correlation using Cu isotopes between leach caps and enrichment blankets. Leach caps have significantly lower amounts of Cu than found in enrichment blankets. As water reacts with chalcopyrite ($CuFeS_2$) found in the primary porphyry and previously leached rocks, Cu is taken into solution and as oxidation produces, creates sulfuric acid. When the ground waters reach the water table, chalcocite (Cu_2S) precipitates from solution, enriching the crust in Cu (Mathur *et al*. 2005).

GEOLOGICAL SETTING

The Silver Bell Mine is located thirty-five miles northwest of Tucson, at an elevation from 2,500 to 3,000ft. The mine consists of four open-pits and is located on 19,000 acres of land (Titley 1994).

The Silver Bell Mine area consists of dipping units that are composed of dacite porphyry, alaskite and monazite. The rock ages span the Paleozoic, Mesozoic and Cenozoic periods. The Paleozoic wall rocks consist of quartzite, siltstone and altered limestone. The carbonate rocks are exposed along the contact between the host rock and intrusions, and host the principal skarn ores in the district. Along the western side of the district, carbonate and other types of rocks have been moved downward by faults, making a basin that has been filled with gravel deposits (Lopez 1995). The thickness of the Paleozoic beds cannot be determined because of faulting and dilation from sills. The Mesozoic host rocks consist of well-sorted and bedded arkose exposed at the southwest corner of the area. Some minor siltstone and conglomerate can also be seen. The Cenozoic intrusive rocks consist of post-mineral, mid-Tertiary andesite and hornblende dykes (Graybeal 1982).

METHODS

Samples were handpicked from both drill cores and directly from the mine pit. The

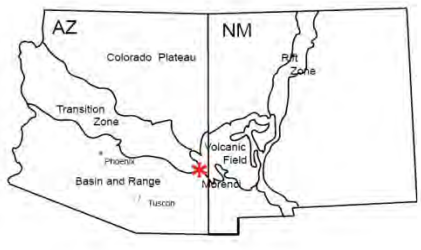

Fig. 1. Map of Arizona

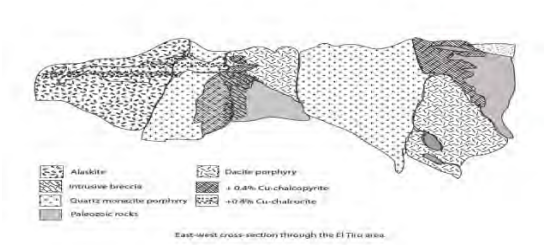

Fig. 2. Cross Section of the Silver Bell Porphyry Cu Mine.

drill core samples were selected from different lithologies to get a representation of the area. In addition, we examined mineralized skarns for evidence of leaching between layers. Minerals from drill cores were crushed and handpicked. Chemical and mineralogical analyses of the ores were conducted on a Scanning Electron Microscope (SEM) and through X-Ray Diffraction (XRD). SEM reveals the mineral replacements throughout the samples, whereas XRD reveals mineralogy. Each of the sections was scanned for places where Cu enrichment could be documented. Minerals were picked for isotopic analysis from each of the samples and confirmed by XRD and SEM.

The rock samples were cut and polished into thin sections to be used on the SEM at Juniata College. The SEM was used for petrographic textural analysis.

Samples were prepared for Cu isotope analysis on the Multicollector Inductively-Coupled Plasma Mass Spectrometer (MC-ICPMS) at University of Arizona. The Cu-rich samples were loaded and dissolved in pure HNO_3 and the Cu-poor samples were loaded and dissolved in a mixture of HCl and HNO_3. Chromatographic separation of the Fe and Cu ions was deemed necessary for the Cu-rich samples. The diluted solutions were injected into the MC-ICPMS using a microconcentric nebulizer. Samples were run numerous times to increase precision. The Cu isotope ratios are reported in conventional per mil notation, relative to the NIST 976 standard. Mass bias was also accounted for by bracketing methods with the NIST 976 standard.

DISCUSSION

The measured Cu isotope ratios vary from -14‰ to 9‰. This range shows that Cu isotope fractionation is significant during supergene leaching and enrichment.

Textural analysis revealed that there have been multiple leach events as recorded in previous studies (Titley 1995). For instance, in the SEM images and analysis of the samples, chalcocite can be seen as a replacement of pyrite. This is evidenced by formation of Cu mineral pseudomorphs after cubic pyrite. Evidence of replacement was seen in many of the samples.

In order to quantify the degree of Cu enrichment, and the number of leach events, we compared the magnitude of Cu isotope fractionation between the enrichment blanket and the leached cap. Relative to primary, hypogene ores, with a δ^{65}Cu value of near 0‰, the Cu isotope fractionation in the enrichment blanket averages 6‰, and in the leach cap, -7‰. The data demonstrate that the degree of isotopic fractionation is large, and its magnitude may correlate with the extent of leaching, as implied in Figure 3.

CONCLUSIONS

Leach caps have a significantly lower amount of Cu than in enrichment blankets due to downward migration and precipitation of leached copper in the form of chalcopyrite ($CuFeS_2$) chalcocite (Cu_2S) and cuprite (CuO).

In the leached cap, hematite is most abundant, followed by jarosite, goethite and malachite. The data from XRD and SEM also reveals that chalcocite is most

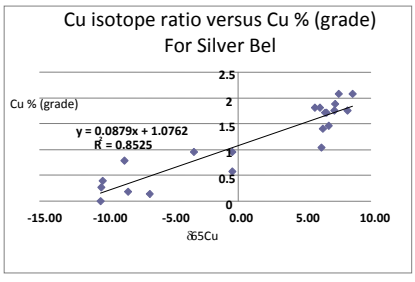

Fig. 3. Cu isotope ratio versus the Cu grade for Silver Bell Mine, Arizona.

abundant followed by cuprite and hematite in the leach cap. This mineralogy can be seen in transition through SEM textures. Samples show replacement of the pyrite by chalcocite, typically found in porphyry Cu deposits.

In the leach cap, the Cu isotopes are lighter than those in the enrichment blanket. Near the surface, the isotopes are extremely low, to about -14‰. Deeper in vertical profile at about 300 feet, the enrichment blanket contains a heavier isotope signature around 8‰. This pattern is observed throughout the drill core. The hypogene mineralization is near 0‰ and therefore, there has been fractionation of copper isotopes in the chalcopyrite during dissolution. This fractionation is seen because the hypogene ores are distinctly different than leach cap and enrichment minerals.

Samples included hematite (Fe_2O_3), goethite (FeO(OH)), and jarosite ($KFe^{(III)}_3(OH)_6(SO_4)_2$) from the leach cap and chalcopyrite ($CuFeS_2$), chalcocite (Cu_2S), and cuprite (Cu_2O) from the enrichment blanket.

REFERENCES

GRAYBEAL, F.T. 1982. Geology of the El Tiro area; Silver Bell mining district, Pima County, Arizona. *Advances in Geology of the Porphyry Copper Deposits: Southwest North America*. University of Arizona Press, Tucson, AZ.

LOPEZ, J.A. & TITLEY, S.R. 1995. Outcrop and Capping Characteristics of the Supergene Sulfide Enrichment at North Silver Bell, Pima County, Arizona. In: PIERCE, W. & BOLM, J.G. (eds.), *Porphyry copper deposits of the American Cordillera: Arizona Geological Society Digest*, **20**, 424-435.

MATHUR, R., RUIZ, J., TITLEY, S., LIERMANN L., BUSS, H., & BRANTLEY, S.L. 2005. Cu isotopic fractionation in the supergene environment with and without bacteria. *Geochimica et Cosmochimica Acta*, **69**, 5233-5246.

TITLEY, S. 1994. Silver Bell Porphyry Copper Deposit, Silver Bell Mountains, Pima County, Arizona. *U.S. Geological Survey Circular* **1103-B**, 77-88.

TITLEY, S. 1995. Geological Summary and Perspective of Porphyry Cu Deposits. In: *Southwestern North America; Porphyry Cu Deposits of the American Cordillera*. Arizona Geological Society Digest, **20**, 6-20.

A geochronological based approach to characterize the setting of the Buffalo Head Hills kimberlite field, northern Alberta, Canada

D. Roy Eccles[1], Art R. Sweet[2], Rob A. Creaser[3], & Larry M. Heaman[3]
[1]*Energy Resource Conservation Board, Alberta Geological Survey, Edmonton, AB CANADA*
(email: roy.eccles@ercb.ca)
[2]*Natural Resources Canada, Geological Survey of Canada, Calgary, AB CANADA*
[3]*Department of Earth & Atmospheric Sciences, University of Alberta, Edmonton, AB CANADA*

ABSTRACT: Chronological studies of kimberlite-host rocks in the diamondiferous Buffalo Head Hills kimberlite field of north-central Alberta facilitate new interpretation of the nature, timing and sequence of kimberlite eruptions in northern Alberta. Three different emplacement episodes are recognized in association with volcanic and intrusive activity: Late Cretaceous (~88-81 Ma) Smoky Group equivalent intra- and extra-crater facies, Late Cretaceous and Paleocene (~81 and ~64 Ma) intrusion of sills or dykes, and Paleocene (~60 Ma) Paskapoo Formation equivalent intra-crater facies. These specific periods of magmatism correspond to characteristic intra-field features such as spatial distribution, rock classification and diamond content.

KEYWORDS: *Alberta, Buffalo Head Hills kimberlite field, Geochronology, Palynology, Kimberlite emplacement setting*

INTRODUCTION

Kimberlite in the Western Canadian Sedimentary Basin (WCSB) has been referred to as 'Class 2 kimberlite' (Skinner & Marsh 2004). A distinct classification is required because these bodies differ from the classical South African carrot-shaped vertical intrusions known as 'pipes', in that Class 2 kimberlites contain large volumes of volcaniclastic rocks deposited in shallow (<500 m in depth) saucer-shaped craters with feeder zones that are often difficult to locate.

The preservation of near-surface to exposed kimberlitic bodies in the Buffalo Head Hills kimberlite field of northern Alberta (Fig. 1) provides an opportunity to contribute to the setting in which Class 2-type kimberlites are emplaced. This information will enhance our ability to model and evaluate known Class 2 kimberlite deposits, and to discover new fields of kimberlite within the WCSB.

Geochronological (radiogenic isotope and palynological) results are used here to understand the kimberlite-host rock relationships in the Buffalo Head Hills kimberlite field, and to provide new philosophy on the timing and distribution of kimberlitic magmatism in the northern Alberta portion of the WCSB.

BACKGROUND

The Buffalo Head Hills kimberlite field is located approximately 350 km north of the city of Edmonton in north-central Alberta. The field was discovered in 1997 by Ashton Mining of Canada Inc., EnCana Corporation and Pure Gold Minerals Inc.

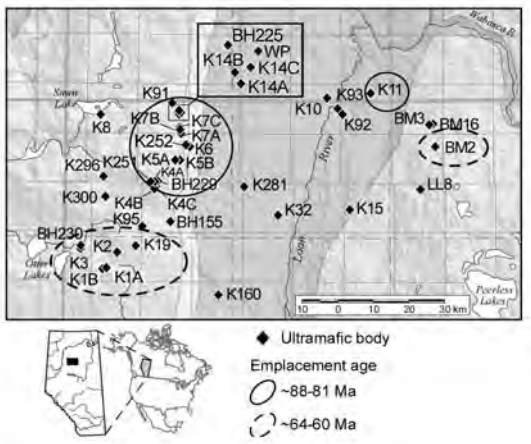

Fig. 1. Spatial location of ~88-81 Ma and ~64-60 Ma ultramafic rocks in the Buffalo Head Hills kimberlite field.

and is currently being explored by Diamondex Resources Ltd., Shore Gold Inc. and Grizzly Diamonds Ltd. This field of 41 known kimberlitic bodies has large near-surface geophysically-inferred kimberlite dimensions (up to and possibly >45 ha), potential economic grades (up to 55 carats per hundred tonnes; K252 kimberlite) and a high ratio of diamondiferous kimberlite to barren hybrid kimberlite-ultrabasic bodies (28 of the 41 occurrences contain diamond; e.g., Skelton *et al*. 2003; Eccles *et al*. 2008).

Examination of drill cores from 21 volcanic bodies provided kimberlite and host rock materials for two separate, but collaborative geochronological studies to understand the timing and distribution of kimberlite magmatism.

(1) Eccles *et al*. (2008) examined kimberlite cores for fresh macroscopic phlogopite and groundmass perovskite and reported robust Rb-Sr (four- to five-point isochrons) and U-Pb (individual $^{206}Pb/^{238}U$ grain data, linear regression, and weighted average $^{206}Pb/^{238}U$) age determinations, respectively, for 12 bodies.

(2) Sweet *et al*. (in prep.) assembled a continuous bedrock section that spans vertically over 560 m to establish the chronostratigraphy and paleoenvironments across the Early Cretaceous (Albian) to Paleocene (Selandian) time-interval most critical for determining the relationship between the configuration of the sedimentary basin and the kimberlite eruptions.

These studies reported two distinctive events: one broadly coeval Turonian to Campanian (~88-81 Ma) volcanism-sedimentation, and the other, a younger Paleocene (~64-60 Ma) eruptive event. Three different emplacement settings are represented, the combination of which defines a complex kimberlite field characterized by tabular, often stacked kimberlite layers of varying ages (Fig. 2).

LATE CRETACEOUS SMOKY GROUP EQUIVALENT INTRA- AND EXTRA-CRATER FACIES

The oldest volcanism in this field is

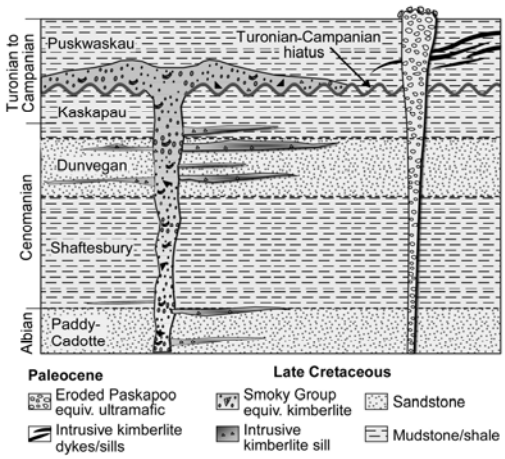

Fig. 2. Cartoon cross-section to depict the complex relations between Late Cretaceous and Paleocene volcaniclastic and intrusive kimberlite in northern Alberta.

recorded by a cluster of Late Cretaceous kimberlites interpreted to be emplaced coevally with Smoky Group host strata. Nine kimberlites yield Coniacian to Campanian ages of between 88 ± 5 Ma (U-Pb perovskite, K5A) and 81.2 ± 2.3 Ma (Rb-Sr phlogopite, K252). The ~88-81 Ma volcanic rocks are bona fide kimberlite (Eccles *et al*. 2004), the majority of which are located in the northwestern part of the field and correspond to a group of diamondiferous bodies, K14, K91 and K252 (Fig. 1), that have the highest diamond contents reported to date for this kimberlite field; these kimberlites have estimated diamond contents of between 12 and 55 carats per hundred tonnes (Skelton *et al*. 2003; Hood & McCandless 2004).

It is difficult to prove these kimberlites are coeval with deposition of Smoky Group sedimentary rocks because an extensive Turonian (in part or in whole) through Early Campanian hiatus, representing approximately nine million years of missing strata, coincides with emplacement. These kimberlites were either covered by post-event Santonian and Campanian strata, or exhumed to outcrop or subcrop beneath glacial deposits. Kimberlite morphologies of this group are complex because their emplacement is controlled by

paleotopography associated with the hiatus (possibly related to tectonic uplift), and subsequently modified as part of a Late Cretaceous landscape that was transgressed by marine waters.

LATE CRETACEOUS AND PALEOCENE INTRUSIVE SILLS AND DYKES

A second emplacement setting is intrusive and occurs as both Late Cretaceous and Paleocene volcanic rocks penetrated significantly older sedimentary rocks.

The Campanian (~81 Ma) K252 kimberlite, which has previously been interpreted as having volcaniclastic textures (Boyer 2005), is reinterpreted here to have, at least partially (i.e., the lower portion of this body), an intrusive origin. The discovery of 'peperitic' textures at an upper kimberlite-mudstone contact provides physical evidence that some of the K252 kimberlite layers were injected as sills into Albian and Cenomanian aged strata (~105 Ma to ~95 Ma). The 'peperite', which is defined by the disintegration of magma intruding and mingling with unconsolidated or poorly consolidated, typically wet sediments (White *et al.* 2000), is characterized by blocky and fluidal textures that include kimberlite-mudstone mingling, fines-depleted elutriation features, and thermally and mechanically-altered mudstone. Jigsaw-fit in-situ fragmentation and mineralized mudstone are also observed at the kimberlite-mudstone contact.

The importance of defining settings for Late Cretaceous volcanic activity in this region is emphasised by new geochronological data that show the two kimberlites with the highest diamond estimates to date, K14 and K252, are included in a 14-point Rb-Sr phlogopite isochron age of 81.5 ± 0.8 Ma (MSWD=0.25).

A much younger intrusive event is associated with the BM2 kimberlite, where Early Paleocene (6-fraction U-Pb perovskite weighted average of 63.5 ± 0.7 Ma) hypabyssal kimberlite intruded into Albian and possibly Cenomanian host rocks. This interpretation is supported by the high thermal maturity indices of palynomorphs derived from the mudstone located directly adjacent to the kimberlite intrusion.

PALEOCENE PASKAPOO EQUIVALENT INTRA-CRATER FACIES

The youngest eruptive event is of Paleocene age (~60 Ma) whereas the youngest preserved host rocks capping the Buffalo Head Hills are of Campanian age (~78 Ma). In this instance, the only record of now eroded latest Campanian through Paleocene host rocks is provided by sedimentary xenoliths preserved in the truncated intra-crater facies ultramafic bodies (e.g., K1 body).

Selandian Rb-Sr ages of 59.6 ± 2.8 Ma and 60.3 ± 0.8 Ma were determined for the K1A and K19 bodies, respectively; these bodies occur in the southwestern part of the field and are either barren of diamond or have the poorest diamond results within this field (Hood & McCandless 2004; Fig 1). Mineralogical (e.g., amphibole, sanidine) and geochemical evidence (e.g., flatter chondrite-normalized REE pattern versus the steep profile of typical kimberlite) enticed Eccles *et al*. (2008) to conclude that these rocks are better referred to as hybrid kimberlite-ultrabasic rocks.

DISCUSSION AND CONCLUSIONS

This new account of the nature, timing and sequence of volcanic eruptions in the Buffalo Head Hills kimberlite field is made possible by improved age determinations. In summary, three different volcanic settings are recognized in the Buffalo Head Hills kimberlite field: Late Cretaceous Smoky Group equivalent intra- and extra-crater facies, Late Cretaceous and Paleocene intrusive sills and/or dykes, and Paleocene Paskapoo Formation equivalent intra-crater facies. Collectively, these episodes define a kimberlite complex characterized by tabular kimberlite layers of varying ages.

In addition to geological modelling, geochronological data has significant implication for diamond exploration. A northern Alberta 'diamond window' occurs

at ~88-81 Ma (Eccles *et al*. 2008) and appears to be prevalent at ~81 Ma.

Because of their proximity (~ 770 km) and similar Class 2 kimberlite designation, some discussion of the similarities and dissimilarities between the Buffalo Head Hills and Fort à la Corne fields is warranted. Both fields are dominated by primary pyroclastic, volcaniclastic and resedimented volcaniclastic kimberlite, and have large, multi-aged bodies. Hence, a favourable consequence to diamond explorers is that the inter- and extra-crater morphologies of Class 2 kimberlite in the WCSB could cover vast areas.

The Fort à la Corne field is significantly older (Albian) than the Buffalo Head Hills field in northern Alberta. However, the intrusion of Campanian (~81 Ma) kimberlite into the Albian Peace River Formation, which is stratigraphically equivalent to Fort à la Corne's Pense and Joli Fou kimberlite deposits, represents the first chronological link between the two fields and raises some enticing notions. As drilling in Alberta has only penetrated depths of about 250 m, it will be interesting to see if deeper exploratory drilling can discover Mannville aged kimberlite in northern Alberta (i.e., equivalent to Fort à la Corne's Cantuar kimberlite). Conversely, it will be interesting to see if any kimberlite layers at Fort à la Corne are intrusive in nature.

A significant dissimilarity between the Buffalo Head Hills and Fort à la Corne fields is the presence of intrusive kimberlite sills and/or dykes in northern Alberta. We propose that intrusive volcanism might occur in the Buffalo Head Hills when: 1) material from an earlier eruption forms a cap-rock at the top of the emplacement pathway and forces subsequent younger eruptions to either break through the now solid cap or penetrate outwards into preferential zones of weakness, and/or 2) the eruption(s) are orceful enough to erupt both vertically and horizontally as the magma nears and breaches the surface.

We further speculate that intrusive kimberlite is preferentially injected into and/or directly adjacent to continental clastic wedges that are representative of major sea level low stands in the WCSB. To resolve the complex issues discussed here, grid-based drilling and large geochronological databases are required.

REFERENCES

BOYER, L.P. 2005. *Kimberlite volcanic facies and eruption in the Buffalo Head Hills, Alberta*. M.Sc. thesis. University of British Columbia.

ECCLES, D.R., HEAMAN, L.M., LUTH, R.W., & CREASER, R.A. 2004. Petrogenesis of the Late Cretaceous northern Alberta kimberlite province. *Lithos*, **77**, 435-459.

ECCLES, D.R., CREASER, R.A., HEAMAN, L.M., & WARD, J. 2008. Rb-Sr and U-Pb geochronology and setting of the Buffalo Head Hills kimberlite field, northern Alberta. *Canadian Journal of Earth Sciences*, **45** (5), 513-529.

HOOD, C.T.S. & MCCANDLESS, T.E. 2004. Systematic variations in xenocryst mineral composition at the province scale, Buffalo Hills kimberlites, Alberta, Canada. *Lithos*, **77**, 733-747.

SKELTON, D., CLEMENTS, B., MCCANDLESS, T.E., HOOD, C. AULBACH, S., DAVIEW, R,. & BOYER, L.P. 2003. The Buffalo Head Hills kimberlite province, Alberta. IN KJARSGAARD, B.A. (ed.), *Slave Province and Northern Alberta Field Trip Guidebook*. Geological Survey of Canada, Miscellaneous Publication G-293.

SKINNER, E.M.W. & MARSH, J.S. 2004. Distinct kimberlite pipe classes with contrasting eruption processes. *Lithos*, **76**, 183-200.

SWEET, A.R., BOYCE, K,. & ECCLES, D.R. In prep. Palynological constraints on kimberlite emplacement models: chronostratigraphy of host rock and clastic xenoliths, Buffalo Head Hills, Alberta.

WHITE, J.D.L., MCPHIE, J., & SKILLING, I.P. 2000. Peperite: a useful genetic term. *Bulletin of Volcanology*, **62**, 65-66.

Nature of $\delta^{18}O_{quartz}$ variation in a Slate-belt – hosted orogenic gold province, Nova Scotia, Canada: evidence for fluid: rock interaction

Daniel J. Kontak[1], T. Kurt Kyser[2], & Rick J. Horne[3]
[1]Depatment of Earth Sciences, Laurentian University, Sudbury, ON, P3E 2C6 CANADA
(e-mail: dkontak@laurentian.ca)
[2]Department of Geological Sciences, Queen's University, Kingston, ON, K7L 3N6 CANADA
[3]Acadian Mining, Halifax, 1969 Lower Water Street, Halifax, NS, B3J 2R CANADA

ABSTRACT: Vein quartz systems in the Meguma gold districts formed during flexural-slip folding of the bedded sandstone-siltstone sequence. Structural studies indicate the concordant (e.g., stratabound, saddle) and discordant (e.g., en echelon) veins represent a single hydrothermal event, but absolute age dating indicates veins formed during regional deformation (410 Ma) and widespread plutonism (380 Ma). Detailed sampling of all vein types at two deposit sites, constrained to 410 and 380 Ma, indicate similar $\delta^{18}O$ values (+15 to +16‰). Thus, fluids of similar $\delta^{18}O$ values were generated at widely different times in the same terrane from different processes. A compilation of $\delta^{18}O_{quartz}$ data for 14 gold districts arranged in their stratigraphic order indicates an upward increasing trend of $\delta^{18}O_{quartz}$ This observed trend can be modeled to result from increasing fluid:rock ratio if an increasing component of chlorite occurs in the wall rock, that is commensurate with the nature of the known composition variation of the stratigraphy up section.

KEYWORDS: *orogenic gold, oxygen isotopes, Meguma Group, Nova Scotia.*

INTRODUCTION

The Meguma Group, Nova Scotia, hosts over 60 past producing gold districts with historic production of >1 M oz. However, recent exploration activity has delineated resources of 0.6-1 M oz at several locations. The Meguma area has been the focus of many studies over the past century and a variety of models proposed for its origin spanning from syngenetic or exhalative, early- to late-stage metamorphic and intrusion-related. Debates on the origin of these and similar slate-belt - hosted vein deposits focused on the origin of the quartz veins and their age of emplacement. Recent structural studies of several gold districts (Horne & Culshaw 2001; Horne & Jodrey 2002) indicate that vein emplacement occurred during the later stages of fold tightening of the host rocks. In this paper, we present results for $\delta^{18}O_{quartz}$ determined for vein samples collected from two well characterized gold districts separated in time by about 30 Ma, compare these data to our earlier studies (Kontak & Kerrich 1995) and model an observed vertical variation of $\delta^{18}O$quartz based on sampling of 14 districts. These data provide further confirmation that: (1) veins in a given deposit represent deposition from a single, isotopically-homogeneous vein-forming fluid; (2) that the source of this fluid is external to the Meguma Group; and (3) that the calculated $\delta^{18}O_{H2O}$ value of the vein-forming fluids reflect variable amounts of fluid:rock interaction.

GEOLOGICAL SETTING

The study area lies within the Meguma Terrane of southern Nova Scotia. The terrane is dominated by the metaturbiditic rocks of the Lower Paleozoic Meguma Group that were intruded at 380 Ma by meta- to peraluminous granitoid bodies. The Meguma Group has a sandstone-rich lower part and siltstone-rich upper part. Deformation and accompanying greenschist to amphibolite grade regional metamorphism occurred at 410-400 Ma. This deformation produced open, upright, northeast-trending folds with shallowly

plunging fold axes. Gold districts occur throughout the lower, sandstone dominant part of the stratigraphy and there is no apparent stratigraphic control, however, the gold districts are localized to structural domes.

DEPOSIT AREAS, VEIN FEATURES & AGE OF FORMATION

Gold districts occur at or proximal to fold hinges where quartz vein density increases dramatically. Vein types include bedding-concordant (i.e., bedding parallel, saddle reefs) and discordant types (en echelon, conjugate) and their mutually cross cutting relations indicate a single vein-forming event. All vein types are observed to contain gold. Horne & Culshaw (2001) argue that the layered Meguma Group rocks were deformed by a flexural-slip fold mechanism and that vein formation was associated with this process. In addition, vein formation also involved periodic fluid overpressures. Importantly, Morelli *et al.* (2005, and references therein) showed that vein formation occurred twice, once at 408 Ma and again at 380 Ma. Veins are dominated by Qtz-Carb-Sulfides (Fe-As) lesser silicates, and other sulfides (Zn Pb, Cu, Bi, Te). A regional zonation of vein mineralogy reflects district proximity to 380 Ma intrusions (Newhouse 1936; Smith & Kontak 1986). Wall rock alteration (e.g., silica, sericite, carbonate, sulfide, tourmaline) is present, but variably developed.

NATURE OF VEIN FORMING FLUIDS

Previous fluid inclusion and isotopic (Sri, $\delta^{18}O$, δD, $\delta^{13}C$, $\delta^{34}S$; Kontak *et al*. 1996; Kontak & Kerrich 1997) studies indicate that fluids were mixed aqueous-carbonic (X_{CO2} = 0.1-0.3), exotic to the Meguma Group, and record variable amounts of fluid:rock interaction. Whereas C and S are dominantly wall rock derived, O isotopic data indicate an external reservoir with subsequent modification.

SAMPLING, ANALYTICAL PROCEDURES

Detailed sampling of all vein types was done in two deposits, The Ovens and Dufferin, where earlier mapping (Horne & Culshaw 2001; Horne & Jodrey 2002) constrains the nature of veins collected. Oxygen was extracted from quartz separates using the BrF_5 technique and isotopic measurements performed using a Finnigan MAT 252 mass spectrometer at Queen's University, Kingston, Ontario. All values are reported using the δ notation in per mil (‰) relative to V-SMOW (Vienna standard mean ocean water, $\delta^{18}O$) and have a precision of ± 0.1 ‰ based on repeated analyses of standards.

ANALYTICAL RESULTS

$\delta^{18}O_{quartz}$ results for the two deposits are very similar regardless of vein types with averages of +15.7 ± 0.6 ‰ (1σ, n=11) for Dufferin and +15.2 ± 0.9 ‰ (1σ, n=15) for The Ovens. In addition, there is limited spread in the data for each area despite different vein types having been analyzed. Thus, although veins are classified based on structural type and appearance (e.g., laminated vs. non-laminated, saddle vs. limb, stratabound vs. discordant), the $\delta^{18}O_{quartz}$ values are the same. In addition, fluid inclusions are similar in quartz from the two areas, with low-salinity (i.e., <6-8 wt% $NaCl_2$ equiv.) aqueous-carbonic (X_{CO2} = 0.1-0.3) types dominant.

DISCUSSION

Several issues are discussed below in order to assess to assess the nature and source of the vein-forming fluids.

$\delta^{18}O$ of Vein-Forming Fluid

The $\delta^{18}O$ values for vein-forming fluids for the two areas sampled are assessed using the $\Delta^{18}O$ (quartz-H_2O) and inferred temperature of vein formation (350-400°C; Fig. 1). The range of $\delta^{18}O_{H2O}$ values is +9 to +12‰ for quartz deposition at 350-400°C. An alternative interpretation is that the variation in $\delta^{18}O_{quartz}$ reflects deposition from a fluid of uniform $\delta^{18}O$, but over a temperature range of about 50°C, as constrained by $\delta^{18}O_{quartz}$ values; it is not possible to discriminate between these models. Regardless, the vein fluids had a

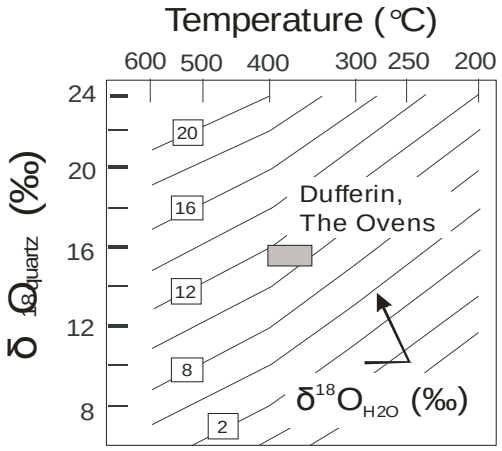

Fig. 1. A plot of δ^{18}Oquartz versus T(°C) with isopleths for $\delta^{18}O_{H2O}$ values of fluids calculated using fractionation equation of Matsuhisa *et al*. (1979). The box outlines the inferred $\delta^{18}O_{H2O}$ values for vein fluids at The Ovens and Dufferin.

uniform $\delta^{18}O_{H2O}$ value of +9 to +12‰. Importantly, the data indicate that a fluid of similar δ^{18}O value can be generated by events separated by 30 Ma within the same geological terrane.

Regional Variation of δ^{18}Oquartz

Analyses of quartz veins from 14 gold districts indicates that there is a limited range in their δ^{18}O values for all vein types in an individual deposit, but a systematic enrichment in $\delta^{18}O_{H2O}$ values is noted when data are arranged stratigraphically in the Meguma Group (Fig. 2), with one deposit area (West Gore) having extreme enrichment. The most primitive $\delta^{18}O_{H2O}$ values occur for deposits at the base of the stratigraphy, with the lowest of these (+9.5‰) for a deposit (Beaver Dam, BD) proximal a 375 Ma granitic intrusion. The observed vertical variation in $\delta^{18}O_{H2O}$ values might be explained by: (1) fluid cooling, (2) fluid mixing, or (3) fluid contamination. The first scenario is eliminated based on previous work indicating that there was no systematic cooling of fluids up section or a change in mineralogy. Case two is discounted, as there is no evidence, such as variable fluid salinity, to indicate fluid mixing occurred. To address contamination of the vein fluid,

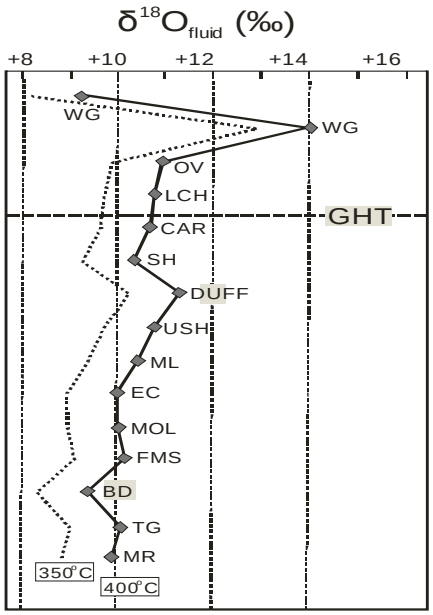

Fig. 2. Plot of $\delta^{18}O_{H2O}$ values (350° and 400°C) for gold districts versus stratigraphic position in the Meguma Group. GHT is the contact between the sandstone dominant Goldenville Fm. And overlying shale dominant Halifax Fm.

we have modeled fluid:rock interaction using appropriate equations in Taylor (1978) and using a primary fluid of +9‰ (see Fig. 2) and an initial whole rock value of +12‰ (Meguma Group value; Longstaffe *et al*. 1980). The calculations indicate that the ^{18}O enrichment of the fluid is possible if a model rock composition contains chlorite and the infiltrating fluid is at 400-500°C. Such a composition is a proxy for the observation of an increasing shale component in Meguma Group higher in the stratigraphy along with a general decrease in metamorphic grade.

SUMMARY AND CONCLUSIONS

Meguma gold-quartz vein deposits were emplaced during regional metamorphism (408 Ma) and peraluminous magmatism (380 Ma) in conjunction with fold tightening of the Meguma Group rocks. Sampling of two well-constrained vein systems formed at these times with the structural features, vein mineralogy and fluid chemistry have identical $\delta^{18}O_{quartz}$ and

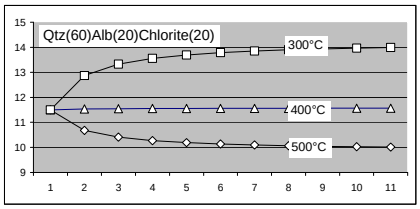

Fig. 3. Plot of fluid:rock ratio versus calculated $\delta^{18}O_{altered\ rock}$ for interaction of fresh rock of known modal composition ($\delta^{18}O$ = +12‰) with fluid of $\delta^{18}O$ = +9‰. Note that a T > 500° is required in order for the fluid to increase its $\delta^{18}O$ value.

indicate $\delta^{18}O_{H2O}$ values of +9 to +12‰ for350-400°C, and suggest a metamorphic fluid. Integration of these data with the $\delta^{18}O_{quartz}$ data for twelve other Meguma deposits indicates a gradual vertical enrichment in $\delta^{18}O$, that is interpreted to have resulted from fluid:rock interaction of a fluid of an initial $\delta^{18}O_{H2O}$ of +9‰ with chlorite-bearing metasedimentary rocks. These conclusions are consistent with other chemical data indicating that the fluids responsible for vein formation are exotic to the Meguma Group.

ACKNOWLEDGEMENTS

This work was funded when the senior author was at the Nova Scotia Department of Natural Resources. Isotopic analyses were also supported by an NSERC Discovery grant to Kyser.

REFERENCES

HORNE, R. & CULSHAW, N. 2001. Flexural-slip folding in the Meguma Group, Nova Scotia. *Journal of Structural Geology*, **23**, 1631-1652.

HORNE, R. & JODREY, M. 2002. Geology of the Dufferin gold deposit (NTS 11D/16), Halifax County. *Nova Scotia Department Natural Resources, Report of Activities 2001*, 51-68.

HORNE, R.J. & PELLY. 2007. Geological transect of the Meguma Terrane from centre Musquodoboit to Tangier. *Nova Scotia Department Natural Resources, Report of Activities 2001*, 71-89.

KONTAK, D.J. & SMITH, P.K. 1989. Sulphur isotopic composition of sulphides from the Beaver Dam and other Meguma Group-hosted gold deposits, Nova Scotia: implications for genetic models. *Canadian Journal of Earth Sciences*, **26**, 1617-1629.

KONTAK, D.J., SMITH, P.K., & HORNE, R.J. 1996. Hydrothermal characterization of the West Gore Au-Sb deposit, Meguma Terrane, Nova Scotia. *Economic Geology*, **91**, 1239-1262.

KONTAK, D.J. & KERRICH, R. 1997. An isotopic (C, O, Sr) study of vein quartz and carbonate from Meguma gold deposits, Nova Scotia, Canada. *Economic Geology,* **92**, 161-180.

LONGSTAFFE, F, SMITH, T.E., & MUELENBACHS, K. 1980. Oxygen isotope evidence for the genesis of Upper Paleozoic granitoids from southwestern Nova Scotia. *Canadian Journal of Earth Sciences,* **17**, 132-141.

MATSUHISA, Y., GOLDSMITH, J.R., & CLAYTON, R.N. 1979. Oxygen isotopic fractionation in the system quartz-albite-anothite-water. *Geochimica et Cosmochimica Acta,* **43**, 1131-1140.

MORELLI, R.M., CREASER, R., SELBY, D., KONTAK, D.J., & HORNE, R.J. 2005. Rhenium-Osmium geochronology of arsenopyrite in Meguma Group gold deposits, Meguma Terrane, Nova Scotia, Canada: Evidence for multiple gold-mineralizing events. *Economic Geology*, **100**, 1229-1242.

NEWHOUSE, W.N. 1936. A zonal gold mineralization in Nova Scotia. *Economic Geology*, **31**, 805-831.

SMITH, P.K. & KONTAK, D.J. 1987. Meguma gold studies: some basic observations. Mines and Minerals Branch *Report of Activities for 1987, Part A., Nova Scotia Department of Mines and Energy, Report* **87-5**, 69-72.

TAYLOR, H.P., Jr. 1978. Oxygen and hydrogen isotope studies of plutonic granitic rocks. *Earth & Planetary Science Letters,* **38**, 177-210.

Tracing progressive redox gradients and directions of hydrothermal flow using uranium and lithium isotopes

Kurt Kyser, Majdi Geagea, Don Chipley, Paul Alexandre, Mark Raycroft, April Vuletich, & Rachel Schwartz-Narbonne

Dept Geological Sciences & Geological Engineering, Queen's University, Kingston, ON CANADA
(e-mail: kyser@geol.queensu.ca)

ABSTRACT: Uranium isotopes fractionate as a result of nuclear volume effects such that $^{238}U/^{235}U$ ratios vary as a function of uranium oxidation state, being highest in reduced species such as U^{4+} in uraninite. The $\delta^{238}U$ values of uranium minerals from volcanic-, metasomatic-, unconformity-, sandstone- and calcrete related uranium deposits worldwide vary by 1.5 ‰ and can be used to indicate sources of uranium. Uraninites with reset ages caused by later recrystallization events have low $\delta^{238}U$ values as a result of mobilization of ^{235}U during interaction with later fluids. Thus, uranium isotopes provide information about source and redox history of the uranium in the deposits.

Lithium isotopes do not fractionate as a result of redox reactions, but ^{7}Li is preferentially partitioned into the fluid phase, whereas ^{6}Li prefers sites in alteration minerals such as micas. The $^{7}Li/^{6}Li$ ratios of mica and chlorite in alteration zones around uranium deposits are higher and decrease to lower values with distance from the ore relative to background mica in the Athabasca Group sandstones. In barren areas, high ratios are rare and background ratios are dominant. When used together, the isotopic composition of uranium and lithium can be utilized to refine both the genesis of uranium deposits and as exploration tools.

KEYWORDS: *Fluid flow path, redox, isotopes*

INTRODUCTION

Variations in the isotopic composition of uranium in uranium ores have only been reported in deposits from Gabon, where natural reactors went critical 2 billion years ago, thereby altering the $^{238}U/^{235}U$ ratio from that reported for all other natural samples (Naudet & Renson 1975; Bros *et al*. 1993). New ICP-MS technologies (Anbar *et al*. 2002) and advances in our understanding of how nuclear structure in the isotopes of some heavy elements can affect bonding have suggested that variations, albeit small, in uranium isotope ratios might occur as a result of redox reactions. These variations occur because nuclei with an odd number of neutrons, such as ^{235}U, have a smaller nucleus relative to nuclei with an even number of neutrons such as ^{238}U, and this difference will result in different bond strengths related to the different sizes of the nuclei. This effect results in differences in $^{238}U/^{235}U$ ratios between phases having different bond types, such as those involving uranium with different oxidation states.

Uranium is a redox sensitive element, with most naturally occurring uranium either as U^{+4} or U^{+6}. Theory would indicate that ^{235}U should be preferentially retained in oxidized phases, such as dissolved U^{+6}, whereas ^{238}U should be preferentially partitioned into reduced species like uraninite (Bigeleisen 1996; Schauble 2007). Thus, most uranium deposits except those associated with high temperature processes should have small variations in their $^{238}U/^{235}U$ ratios as a result of the extent that a pool of uranium is reduced from U^{+6} to U^{+4}.

As predicted from the nuclear size effect on the distribution of uranium isotopes, Sterling *et al*. (2007) and Weyer *et al*. (2008) report a total variation of 1.5 ‰ in the $^{238}U/^{235}U$ ratios decreasing in the order from black shales > basalts, > seawater, > banded iron formations (BIFs). The black shales reflect preferential reduction by organic matter of ^{238}U from seawater,

basalts reflect reducing, high-temperature environments and BIFs reflect the preferential adsorption of ^{235}U from seawater by Fe-oxides (Weyer *et al*. 2008). Bopp *et al*., (2008) report that $^{238}U/^{235}U$ ratios in sandstone-type uranium ores are greater than magmatic uranium ores by 1 ‰, but no explanation for this difference was proposed other than a reflection of different redox conditions.

In marked contrast to the chemical behaviour of U, Li is not redox sensitive so that variations in its isotopic composition will not reflect the redox process associated with deposits. However, the 17% mass difference between the ^{6}Li and ^{7}Li is significant so that fractionation of Li as it changes bonding environment should be substantial. The light isotope ^{6}Li preferentially enters solid phases, so that the $^{7}Li/^{6}Li$ ratio in a hydrothermal fluid should increase upstream, as should the ratios in the alteration minerals that result from this fluid (Millot *et al.* 2007). The $^{7}Li/^{6}Li$ ratio in alteration minerals should increase towards the deposit along the flow path of the mineralizing fluid (Millot & Negrel 2007). Thus, Li isotopes might be indicators of the direction of fluid flow in mineralizing systems.

RESULTS

Uranium Isotopes

The $^{238}U/^{235}U$ ratios of uranium minerals from volcanic-, metasomatic-, unconformity- and sandstone-related uranium showings and deposits worldwide measured by multi-collector ICP-MS indicate a total variation in $\delta^{238}U$ values of 1.5 ‰, with the $^{238}U/^{235}U$ ratio varying as a function of type of uranium deposit (Fig. 1).

Because of the high temperatures involved in magmatic- and metasomatic-related uranium deposits, variations in their $^{238}U/^{235}U$ ratios should be minimal, unless later alteration has resulted in mobilization of uranium. The calcrete deposits measured so far (Fig. 1) are known to have uranium derived from a near-by igneous source, and they have $^{238}U/^{235}U$ ratios in carnotite consistent with such a source. Metasomatic-related

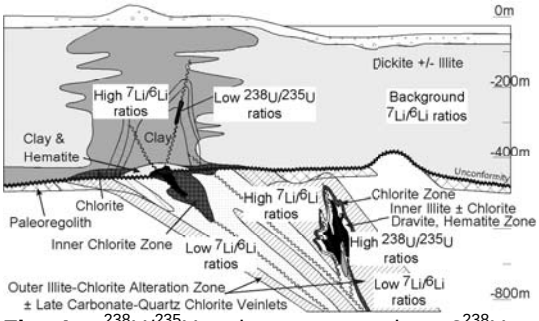

Fig. 1. $^{238}U/^{235}U$ ratios, expressed as $\delta^{238}U$ values, of uraninite ores from different classes of uranium deposits. Within the unconformity-related deposits, complex-type deposits have the lowest $^{238}U/^{235}U$ ratios whereas simple types have higher ratios. Also shown is the range of $^{238}U/^{235}U$ ratios in basalts/granites and sediments.

deposits also have $^{238}U/^{235}U$ ratios consistent with a dominantly igneous-related source.

Unconformity-type uranium deposits, as well as sandstone-hosted deposits, should be zoned in their $^{238}U/^{235}U$ ratios as a result of two processes. In the first process, the $^{238}U/^{235}U$ ratios in the first uraninite precipitated should be greatest and should decrease as the ^{238}U is preferentially removed from the fluid. This process will result in a gradient of $^{238}U/^{235}U$ ratios such that we would expect the highest ratios distal from the redox centre and within the redox centre we would expect lower ratios (Fig. 2). The other process that could affect the ratios would involve mobilization of uranium by later fluids. If these fluids are oxidizing, as they must be to mobilize the ore, we would expect ^{235}U to be preferentially partitioned into the fluid phase. Indeed, in some basement-hosted deposits, uraninite with the lowest apparent ages have the lowest $\delta^{238}U$ values as a result of ^{235}U being preferentially mobilized into secondary fractures. This ^{235}U could then be absorbed by iron oxides and other phases or precipitated as secondary minerals, resulting in $^{238}U/^{235}U$ ratios that decrease away from the ore zone. This uranium is extractable using a weak acid leach and can be used to vector into high-grade ore, and should be applicable to all

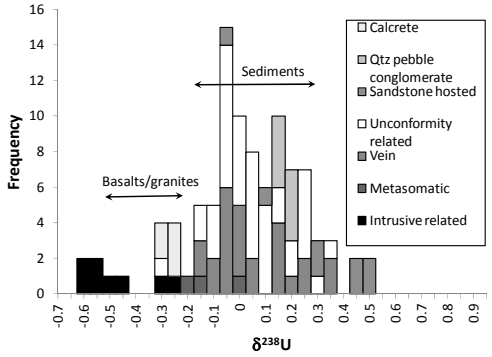

Fig. 2. General alteration and geologic features of basement- and sandstone-hosted uranium deposits showing distributions in U and Li isotope ratios.

uranium deposit types.

Lithium Isotopes

The $^{7}Li/^{6}Li$ ratios in muscovite and chlorite alteration proximal and distal to uranium deposits in the western Athabasca Basin and in barren systems in the eastern Athabasca Basin are highest in the ore zone and decrease in the basement rocks and lower Athabasca Group sandstones further away from the mineralized zone. In barren areas, high ratios are rare and background ratios are dominant. We interpret lower $^{7}Li/^{6}Li$ ratios to reflect the ingress of hydrothermal fluids associated with alteration and mineralizing events and the highest ratios as the down-stream portions of these systems, that have become enriched in ^{7}Li. If valid, $^{7}Li/^{6}Li$ ratios would indicate where in the hydrothermal systems the muscovite and chlorite alteration is located because fluids associated with the ore forming process involve the highest degree of interaction with rocks to become enriched in ^{7}Li.

CONCLUSIONS

$^{238}U/^{235}U$ ratios, expressed as $\delta^{238}U$ values, of uraninite ores from different classes of uranium deposits vary widely. These variations reflect a combination of the source of the uranium, the efficiency of the redox environment in which the minerals were precipitated and the degree that uranium was previously removed from the mineralizing fluid. Therefore, uranium isotopes can be used to refine the critical processes in the generation of uranium deposits, as well as indicate proximity to an ore forming environment.

$^{7}Li/^{6}Li$ ratios in muscovite and chlorite associated with uranium mineralizing events are distinct from background ratios, with the lowest values reflecting the beginning of hydrothermal alteration systems whereas the highest values are indicative of the terminal flow of hydrothermal fluids. Together, these two systems can be used to vector to ore-forming environments. Identification of proxies in elemental concentrations for these two isotope systems might result in an effective exploration tool as a vector for uranium deposits, particularly those in sedimentary basins.

ACKNOWLEDGEMENTS

We thank Cameco Corp., Uravan Minerals, Strateco Resources and the Royal Ontario Museum for samples used in this study.

REFERENCES

ANBAR, A.D., ARNOLD, G.L., RYE, R., & WEYER, S. 2002. Iron isotopes in an Archean Paleosol; Abstracts of the 12th annual V. M. Goldschmidt conference. *Geochimica et Cosmochimica Acta,* **66**(15A), 18.

BIGELEISEN J. 1996. Temperature dependence of the isotope chemistry of the heavy elements. *Proceedings of the National Academy of Sciences,* **93**, 9393-9396.

BROS, R., TURPIN, L., GAUTHIER-LAFAYE, F., HOLLIGER, P., & STILLE, P. 1993. Occurrence of naturally enriched (super 235) U; implications for plutonium behaviour in natural environments. *Geochimica et Cosmochimica Acta,* **57**, 1351-1356.

KYSER, T.K., CHIPLEY, D., VULETICH, A., & ALEXANDRE, P. 2008. Variations in 238U/235U ratios in natural uranium ore minerals from sedimentary basins; Abstracts of the 18th annual V. M. Goldschmidt conference. *Geochimica et Cosmochimica Acta,* **72**(12), A508.

MILLOT, R. & NEGREL, P. 2007. Multi-isotopic tracing (delta (super 7) Li, delta (super 11) B, (super 87) Sr/ (super 86) Sr) and chemical geothermometry; evidence from hydro-geothermal systems in France. *Chemical Geology,* **244**, 664-678.

MILLOT, R., NEGREL, P., & SANJUAN, B. 2007. Lithium isotopes in geothermal systems; Abstracts of the 17th annual V. M. Goldschmidt conference. *Geochimica et Cosmochimica Acta,* **71(**15S), A667.

NAUDET, R. & RENSON, C. 1975. Resultats des analyses systematiques de teneurs isotopiques de l'uranium. Results of systematic analyses of isotopic content of uranium. In: *Le phenomene d'Oklo--The Oklo phenomenon* Internatinal Atomic Energy Agency, Vienna, Austria (AUT).

SCHAUBLE, E.A. 2007. Role of nuclear volume in driving equilibrium stable isotope fractionation of mercury, thallium, and other very heavy elements. *Geochimica et Cosmochimica Acta,* **71**, 2170-2189.

STIRLING, C.H., ANDERSEN, M.B., POTTER E.-K., & HALLIDAY, A.N. 2007. Low-temperature isotopic fractionation of uranium. *Earth and Planetary Science Letters,* **264**, 208-225.

WEYER, S., ANBAR, A.D., GERDES, A., GORDON, G.W., ALGEO, T.J., & BOYLE, E.A. 2008. Natural fractionation of (super 238) U/ (super 235) U. *Geochimica et Cosmochimica Acta,* **72**, 345-359.

The use of Cu isotope fractionation in low temperature ore systems as a geochemical exploration tool

Ryan Mathur[1], Spencer R. Titley[2], Susan Brantley[3], & Marc Wilson[4]
[1]*Juniata College, Huntingdon, PA USA (e-mail: mathur@juniata.edu)*
[2] *University of Arizona, Tucson, AZ USA*
[3]*Pennsylvania State University, State College, PA USA*
[4]*Carnegie Museum of Natural History, Pittsburgh, PA USA*

ABSTRACT: On the surface of the earth highly weathered deposits are characterized by Fe-oxides that represent the weathered remnants of sulfide mineralization, it is difficult to find and assess potential enrichment at depth. In order to assess the importance of leaching and enrichment of mineral deposits, Cu isotope geochemical analyses of leach cap and enrichment minerals can provide important information about current and past supergene processes. We examine copper isotope fractionation in actively weathering soils, epithermal, porphyry copper and massive sulfide deposits from around the world. A distinct pattern of isotopically depleted weathered/leached minerals at the surface and isotopically enriched enrichment exists for all types of deposits. Patterns of isotopic fractionation and the magnitude of isotopic fractionation might suggest where the deposit could be located as well as the degree of weathering history (i.e., few vs. multiple leach events). Because the patterns of copper isotope fractionation are identical regardless of geologic environment, copper isotope analysis provides a technique for understanding supergene processes worldwide.

KEYWORDS: *Cu isotopes, porphyry copper, supergene*

INTRODUCTION

Understanding supergene processes and their impact on any deposit type is essential for mineral assessment. The degree or amount of weathering of porphyry copper deposits, massive sulfide deposits, or any sedimentary-related deposits will directly impact the concentration of metals found in the deposit. Conventional dating of supergene minerals indicates that weathering occurs over the span of millions of year, whereas some deposits show little evidence of supergene activity when drilled at depth.

In this contribution, the fractionation of Cu isotopes during the aqueous low temperature reactions aids in identification of the minerals involved in weathering and the extent of weathering in area.

The supergene environment is an ideal place to document the effects of copper isotope fractionation in the weathering cycles of ore deposits. As is the case with light stable isotopes (O, S, N, and C) copper isotopes are thought to fractionate due to quantum mechanical effects associated with different vibrational frequencies associated with bonding (Seo *et al*. 2007). Models predicting fractionation of copper isotopes at both high temperatures (>300^{o}C of ca. 0.5‰) and low temperatures (<50^{o}C with approximately 3‰ fractionation) have been recently constructed (Seo *et al*. 2007). If multiple stages of low temperature leaching (progressive weathering of enrichment blankets) occurred; copper isotope fractionation in the leached caps and enrichment blankets could be on the order of several tens per mil. Other causes that could impact the degree of fractionation such as crystallography, pH, Eh, and temperature of these isotopes have been and are currently being investigated by (Wall *et al*. 2007). In this study, we focus on the copper isotope composition of the residual reactants and the products of sulfideweathering in nature.

GEOLOGICAL SETTING

Weathering of sulfide-rich rocks from

porphyry copper deposits, massive sulfidedeposits and sulphide-bearing black shale from around the world provide global and diverse geologic perspectives of the utility of Cu isotope fractionation as an exploration tool.

In general, the emplacement processes of the ore deposits results in the development of intensely shattered (permeable) rock volume through which hydrothermal fluids flow, depositing both sulfide and silicate minerals, but most importantly in the context here, pyrite (FeS_2) and chalcopyrite ($CuFeS_2$). When the primary system is unroofed or exposed at or near the surface, and above a lowered water table, oxidizing waters and biogenic activity generate acid from the decomposition of pyrite. The acidic and oxidizing solutions dissolve copper sulphides (like chalcopyrite) and move copper in solution down to a level where free oxygen is diminished, generally considered the top of the water table. Progressive neutralization of the supergene fluids through hydrogen consumption in reaction with host rocks forms supergene silicate alteration minerals and chalcocite.

The processes result in the separation of levels in the supergene profile, the zone of *oxidation* downwards grades into a zone of *leaching,* then into a zone of *enrichment*.

During soil generation, the breakdown of rock to soil mimics the general supergene process described above with the oxidation of rock, formation of clays and the generation of oxide minerals.

METHODS

Samples are from drill core, hand specimens, or augered core. The samples are composed of oxide or sulfidefor the ore deposit samples. The soil samples are mixtures of oxides and silicates. Approx. 0.05g of powdered sample material was dissolved in aqua-regia over night at 200˚C and dried on a hot plate at 40˚C. Cu was separated from the matrix through ion exchange chromatography (IEC) as outlined in Mathur *et al*. (2005) without the use of hydrogen peroxide. To ensure all of the Cu was recovered, gravimetric yields were checked for IEC samples and only samples with >90% yield are reported.

The samples purified with IEC were diluted to approximately 100 ppb Cu. These samples were injected into a Multicollector Inductively-Coupled-Plasma mass spectrometer (MC-ICPMS, Micromass Isoprobe at the University of Arizona and Neptune at Washington State University) in low resolution mode using a microconcentric nebulizer to increase sensitivity for the samples with lower concentrations of copper. The nebulizer flow was adjusted so that the intensity of the ^{63}Cu beam remained constant at 2 volts. Both on and off peak blank corrections were applied to the data and yielded the same result.

Copper isotope ratios are reported in the familiar delta notation:

$$\delta^{65}Cu\ (‰) = \left\{ \left(\frac{\left(\frac{^{65}Cu}{^{63}Cu}\right)_{sample}}{\left(\frac{^{65}Cu}{^{63}Cu}\right)_{standard}} \right) - 1 \right\} * 1000 \quad (1)$$

where the standard was the NIST 976 Cu standard. Two blocks of 25 ratios are reported as an average for each run. Within each run, the measurement error for $\delta^{65}Cu$ was less than 0.01‰ for all analyses.

A major concern surrounding isotope data obtained during analysis is the measurement error associated with mass fractionation within the instrument owing to variations in operating conditions (e.g. Marechal *et al*. 1999). In order to constrain the errors associated with copper isotope analyses on our instrument, we compared all of the copper ratios to the NIST 976 copper standard (eq. 1) using standard-sample-standard bracketing. The 2σ error for the variation of the standard for eight analytical sessions was observed to be $\pm$ 0.14‰.

DISCUSSION

Figure 1 plots all of the data from the ore deposits. Notice that primary high

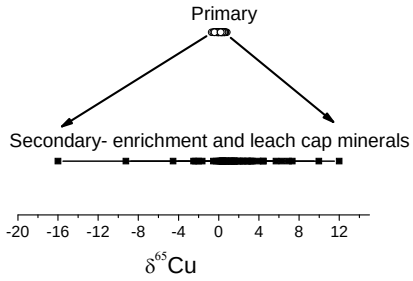

Fig. 1. Plot of δ^{65}Cu values for primary and secondary copper minerals. Data taken from Mathur *et al*. (2009), Aseal *et al*. (2007), Markl *et al*. (2005), Mathur *et al*. (2005), Larson *et al*. (2003), and this study.

temperature mineralization has a relatively tight cluster of δ^{65}Cu, whereas enrichment and leach cap minerals span over 28‰. Thus, aqueous low temperature geochemical reactions result in large variations of the Cu isotope composition in rocks.

Three different isotope reservoirs characterize the weathering process in ore deposits:

(1) High temperature, primary mineralization
(2) Leached rock
(3) Enriched rock

Each reservoir possesses a distinct isotopic signature. Several studies have demonstrated the impact of oxidation during weathering of primary sulphides. The oxidized product favours the heavy isotope, whereas the reduced residual material favours the lighter isotope. The relationship leads to the generation of distinct leach cap, enrichment and primary isotope signatures portrayed in Figure 2.

The data provides two general types of information: an indication of the degree of weathering in an area and the types of Cu minerals that weathered to generate the Cu isotope signatures present.

In order to quantify the degree of leaching that occurred during weathering, the following expression is used:

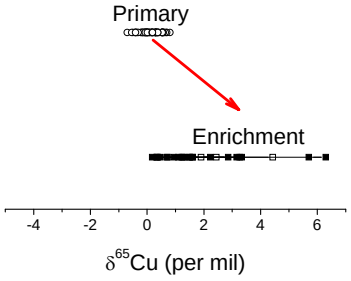

Fig. 2. Plot of primary chalcopyrite and secondary chalcocite data taken from the same sources as Figure 1.

$$\Delta=\delta^{65}\mathrm{Cu}_{\text{ secondary Cu mineral}}-\delta^{65}\mathrm{Cu}_{\text{primary Cu mineral}} \quad (2)$$

In theory, greater values of Δ^{65}Cu indicate greater degrees of leaching because each leach involves oxidation and reduction reactions that increase the fractionation of copper isotopes between secondary copper minerals. The equation could compare the primary sulfideto the leach cap value (this is what is done with the Marcellus soil sample) to obtain a value that indicates the degree of weathering. Both assume that leached Cu from the leach cap migrated downward without any lateral loss of Cu (for instance Cu rich waters laterally migrating to form exotic Cu deposits or that the groundwaters drained into a larger body of water). The values reported are the average copper isotope signature of each reservoir; in order to fairly assess the degree of leaching within a deposit, larger sampling sizes are necessary. Nonetheless, Mathur *et al*. (2005) modelled this behaviour with Rayleigh fractionation trends and positive Δ values further demonstrated that sequential leaching during weathering can lead to highly fractionated Cu isotope ratios in productive porphyry copper systems as demonstrated in Table 1.

The Δ^{65}Cu values greater than 1 correlate with deposits that have well developed enrichment blankets, whereas deposits with lower values such as Butte,

Table 1. Results from Mathur *et al*. (in print), Borg *et al*. (2009), and this study.

Deposit	$\Delta_{secondary\text{-}primary}$
Chuquicamata, Chile	1.85‰
El Salvador, Chile	2.33‰
Collahuasi, Chile	2.49‰
Morenci, USA	2.1‰
Butte, USA	0.38‰
Sliver Bell, USA	5.14‰
Skorpion, Nambia	0.60 ‰
Marcellus Soils	0.43‰

Skorpion and the Marcellus soils correlate with areas that have not experienced much secondary copper enrichment.

In order to develop larger Δ^{65}Cu values, reactions involving large fractionation factors or multiple leach events are necessary. Experimental work from Kimball *et al*. (in print) and Wall *et al.* (2007) defined fractionation factors during the oxidative dissolution of several Cu sulfides. The dissolution of chalcocite generated the largest fractionation factor with values at 2.5 to 3.6 in comparison to 0.8 to 1.6 for the other 7 sulfide analyzed. Thus, larger degrees of Cu isotope separation between the three isotopic reservoirs could indicate the construction and destruction of chalcocite enrichment blankets.

The exploration potential resides in the ability to find leach caps with lighter isotopic compositions that could indicate areas of leaching, or chalcocite samples that have heavier isotope compositions that correlate with multiple cycles of enrichment.

CONCLUSIONS

In summary, the dataset indicates:

(1) Leach cap expressions on the surface reflect what could be beneath in these porphyry copper systems.

(2) Cu isotope compositions of chalcocite from enrichment blankets or Fe-oxides from leach cap minerals could indicate the degree of leaching.

(3) The copper isotope composition of waters actively weathering copper minerals could have distinctly heavy copper isotope signatures and indicate areas where highly enriched ore exist.

ACKNOWLEDGEMENTS

This material is based upon work supported by the National Science Foundation under Grant No. CHE-0431328. We would like to thank Asarco, Codelco and Phelps Dodge for permission to sample and financial support.

REFERENCES

ASEAL, D. MATTHEWS, A., BAR-MATTHEWS, M., & HALICZ, L.. 2007. Copper isotope fractionation in sedimentary copper mineralization (Timna Valley, Israel). *Chemical Geology*, **243**(3-4), 238-254.

KIMBALL, B., *et al.* (in print) Copper isotope fractionation in acid mine drainage. *Geochimica et Cosmochimica Acta*

LARSON, P.B. *et al*. 2002. Cu isotopes; tracing metal sources in ore deposits. *Geochimica et Cosmochimica Acta*, **66**(15A), 432.

MARKL, G., LAHAYE, Y., & SCHWINN, G. 2006. Copper isotopes as monitors of redox processes in hydrothermal mineralization. *Geochimica et Cosmochimica Acta*, **70**(16), 4215-4228.

MATHUR, R. *et al*. 2005. Cu isotopic fractionation in the supergene environment with and without bacteria. *Geochimica et Cosmochimica Acta*, **69**(22), 5233-5246.

MATHUR *R., et al*. (in print) Exploration potential of Cu isotope fractionation in Porphyry Copper deposits. *Journal of Geochemical Exploration*.

SEO, J.H., LEE, S.K., & LEE, I. 2007. Quantum chemical calculations of equilibrium copper (I) isotope fractionations in ore-forming fluids. *Chemical Geology*, **243**, 225-237.

WALL, A., HEANEY, P., MATHUR, R. 2007. Insights into copper isotope fractionation during the oxidative phase transition of chalcocite, using time-resolved synchrontron X-ray diffraction. *Geochimica Cosmochimica Acta,* **77**, A1081.

Oxygen isotope zoning in subvolcanic, intrusion-centered submarine hydrothermal systems as a guide to VMS exploration

Bruce E. Taylor[1], Greg Holk[2], Benôit Dubé[3], & Alan Galley[1]
[1] *Geological Survey of Canada, Ottawa, ON, K1A 0E8 CANADA (btaylor@nrcan.gc.ca)*
[2] *Department of Geological Sciences, California State University, Long Beach, CA, 90840-39002 USA*
[3] *Geological Survey of Canada, Québec, QC, G1K 9A9 CANADA*

ABSTRACT: Oxygen isotope mapping (previous and on-going) about four sub-volcanic intrusive centers in Canada (Clifford-Ben Nevis and Sturgeon Lake, Ontario; Noranda, Quebec; and Snow Lake, Manitoba) and in Sweden (Kristineberg), among others, has revealed a number of systematics that can be applied to the exploration of volcanic-associated massive sulfide(VMS) deposits. Isotope analysis acquired of >2500 whole-rock samples, plus >600 analyses from the literature, has facilitated mapping of paleo-hydrothermal systems covering from 84 km^2 (Snow Lake) to 525 km^2 (Noranda), with sample densities (samples/km) of 1.5 (Clifford-Ben Nevis) to 10.6 (Snow Lake). In simple systems, VMS deposits occur in isotopically "normal" rocks, between semi-conformable zones of low- and high-δ^{18}O values representing, respectively, the high-temperature reaction zone, and either later, hanging wall alteration during waning hydrothermal activity, or unaltered, post-VMS rocks. Recognition of both zones provides a means of assessing an area, and an exploration vector. Discordant alteration along synvolcanic faults provides a local exploration guide. Superposition of single-phase systems by successive magmatic emplacement and hydrothermal activity leads to multi-phased alteration, higher water/rock ratios and more productive areas. An apparent, positive correlation between district VMS tonnage, and aerial extent of synvolcanic intrusions and low δ^{18}O zones, suggests a means of quantitative terrane assessment.

KEYWORDS: *Subvolcanic, VMS, exploration, oxygen isotopes, hydrothermal system*

INTRODUCTION

Volcanic-associated massive sulfide (VMS) deposits that form at or near the seafloor in submarine, magmatic-centred hydrothermal systems contain altered rocks whose oxygen isotope characteristics provide a robust fingerprint of economic import. The application of oxygen isotope mapping to delineate large magmatic-centered hydrothermal systems has been described by a number of authors since the classic work of H. P. Taylor and co-workers (e.g., H. P. Taylor 1974). With few exceptions (e.g., Criss *et al*. 2000; Cathles 1993; Criss & Taylor 1983), however, the areas covered and the sample densities involved in these studies were necessarily restricted. A GSC-CAMIRO project (Galley *et al*. 2002) and current TGI-III Abitibi project (GSC-Quebec-Ontario) have afforded comparative study of several complex sub-marine magmatic-hydrothermal systems on a sufficiently large scale that some new important, general aspects have emerged. Additionally, oxygen isotope techniques used to detect, delineate and quantify submarine hydrothermal systems offer an advantage over more classical lithogeochemical techniques because the record of isotopic alteration can survive to anatexis.

GEOLOGICAL SETTING

Three mineralized districts in Canada containing trondhjemitic to tonalitic subvolcanic complexes of variable size have been iso-topically mapped: Snow Lake, Manitoba (84 km^2); Sturgeon Lake, Ontario (175 km^2); and Noranda, Quebec (>525 km^2); and one in Sweden: Kristineberg mine area, Skellefte district (90 km^2). The Clifford stock, a sub-volcanic intrusion without known associated VMS deposits in the Clifford-Ben Nevis townships, Ontario (160 km^2),

west of Noranda, originally selected as a control case, is now known to post date enclosing volcanic rocks by ca 10 Ma (Piercey *et al*. 2008). Current studies in the Blake River Group extend our knowledge eastward from Noranda (2704-2699 Ma), to the highly fertile Doyon-Bousquet-LaRonde Au-rich VMS district (2699-2695 Ma; McNicoll *et al.* 2008). The derived general isotopic systematics apply, in spite of differences in metamorphism, deformation, and magmatic and hydrothermal complexity.

ANALYTICAL METHODS

Representative hand samples, free of mega-scopic veining and weathered surfaces were analyzed for their oxygen isotope composi-tions using standard fluorination procedures employing BrF_5 (Clayton & Mayeda 1963; Taylor 2004), yielding ca.100 µmole-sized samples of CO_2 for isotope-ratio mass spectrometry in a Finnigan MAT252 mass spectrometer. The oxygen isotope data are reported using standard δ-notation in permil (‰), relative to V-SMOW. The routine value for NBS-28 obtained in the GSC-LSI laboratory (Ottawa) is 9.5 ‰. The precision of $\delta^{18}O$ values reported for whole-rock samples in this study is better than 0.2 ‰.

The sample densities (samples/km^2) for areas not highly-strained are: Clifford-Ben Nevis (1.5), Noranda (1.8), and Sturgeon Lake (2.6). Areas with marked folding, high strain, synvolcanic faults, and intrusive contacts are best sampled locally with closer spacing (e.g., Snow Lake, 10.6 samples/km^2). Availability of outcrop and drill core determines uniformity of sample coverage.

RESULTS AND DISCUSSION

The plot of $\delta^{18}O$ versus the integrated, water/rock ratio (e.g., Criss & Taylor 1986) in Figure 1 graphically describes isotopic alteration of two model rock types, andesite (A, primary $\delta^{18}O$ = 6.0 ‰) and rhyolite (R, primary $\delta^{18}O$ = 7.0 ‰), simply modeled by feldspar-seawater ($\delta^{18}O_{SW}$ = 0.0 ‰), over a wide range of water/rock

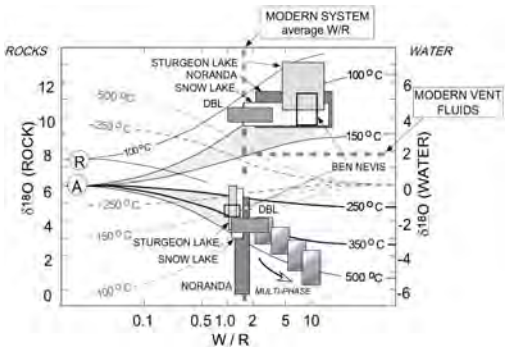

Fig. 1. Water/rock reaction diagramme illustrates fields of mapped high- and low-temperature isotopic alteration (see text) for rhyolites (R) and andesites (A) districts studied (DBL = Doyon-Bousquet-LaRonde). Solid and dashed curves: evolution of rock and water, respectively. Multi-phase reaction history of the central Noranda district, shown schematically, generally corresponds to intrusive history. Approximate $\delta^{18}O$ of modern high-temperature submarine vent fluid and estimated W/R after Shanks *et al*. (1995) and Bowers & Taylor (1985), respectively.

ratios at water/rock ratios of ca. 1 to 2 (e.g., see Shanks *et al.* 1995) to yield the average isotopic compositions for low- and high-temperature altered rocks shown for each district. The fields of data in Figure 1 corresponds to those used to map zones of high- and low $\delta^{18}O$, i.e., areas of low- and high-temperature alteration, respectively. Differences in plotted positions of data fields reflect significant contrasts in the hydrothermal and non-hydrothermal alteration histories in each area. In Noranda, for example, altered rocks bear the effects of multiple, superposed hydrothermal systems.

Marked differences in whole-rock $\delta^{18}O$ values are acquired during water/rock interaction due to variation in temperature (Fig. 1). Contour maps of whole-rock $\delta^{18}O$ record cumulative paleo-heat and fluid flow.

Isotopic mapping of five selected areas in Canada and Sweden has indicated that the isotopic zones ($\delta^{18}O$ <6‰ and >9‰; separate fields, Fig. 1) are not fully coeval. Values of $\delta^{18}O$ ≥9‰ in hanging wall rocks largely indicate waning temperature and fluid flow, and post-date much of the high

temperature ($\delta^{18}O$ < 6.0 ‰), reaction zone alteration. Relative timing of hydrothermal activity and hanging-wall deposition is a key factor in recorded vertical isotopic gradient.

Paired high-low $\delta^{18}O$ patterns can provide a regionally applicable exploration guide: VMS deposits are located in 'normal' isotopic zones, between conformable low- and high$\delta^{18}O$ zones (Fig. 2A-C). Discordant zones of isotopic alteration mark up-flow, typically along syn- volcanic faults, beneath VMS deposits.

SUMMARY

Key features of the selected districts (Fig. 3) include: Noranda: composite, mulitphase high-temperature zone above Flavrian intrusive complex; VMS deposits associated with up-flow zones; Sturgeon Lake: single hydrothermal phase, area eventually emergent resurgent Biedelman Bay tonalite post-dated hydrothermal activity; Snow Lake: two magmatic cycles, each with hydrothermal systems; regionally metamorphosed; Kristineberg: two principal magmatic-hydro-thermal phases, regionally metamorphosed; Ben Nevis: younger, upright stock; single hydrothermal phase; no known VMS deposits.

ACKNOWLEDGEMENTS

The late Adrian Timbal provided invaluable analytical assistance during the GSC-CAMIRO project.

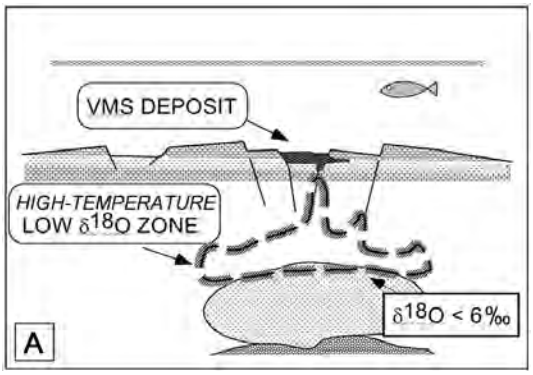

Fig. 2a. Schematic cross section of simple magmatic-centred hydrothermal system. Rocks within high-temperature (e.g., >350 °C) reaction zone are characterized by low values of $\delta^{18}O$.

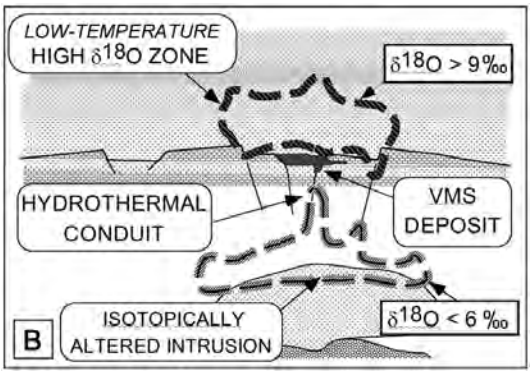

Fig. 2b. Where deposition continues post-VMS, cooling, fluids from the buried hydrothermal system can produce high-$\delta^{18}O$ zones in the hanging wall above up-flow conduits.

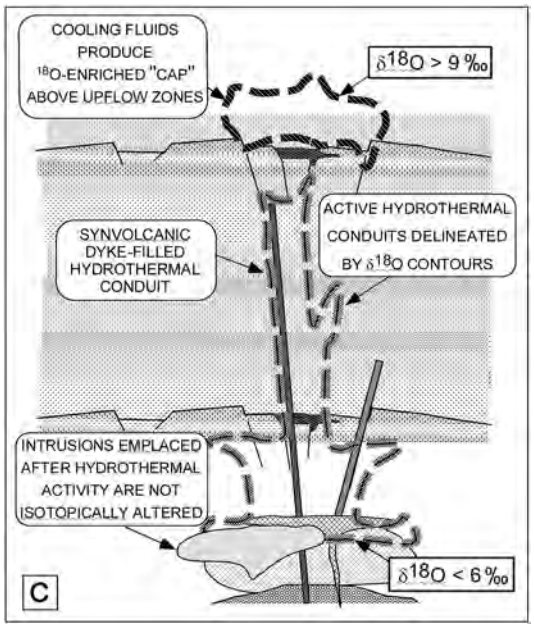

Fig. 2c. Successive intrusive episodes associated with hydrothermal activity can produce compound zones of isotopically altered rocks. The outer O-isotope isopleth is the youngest feature of the reaction zone, and the high $\delta^{18}O$ zone in the hanging wall, the youngest alteration feature overall. Post-hydrothermal intrusions usually lack oxygen isotope alteration.

REFERENCES

CATHLES, L.M. 1993. Oxygen isotope alteration in the Noranda mining district, Abitibi

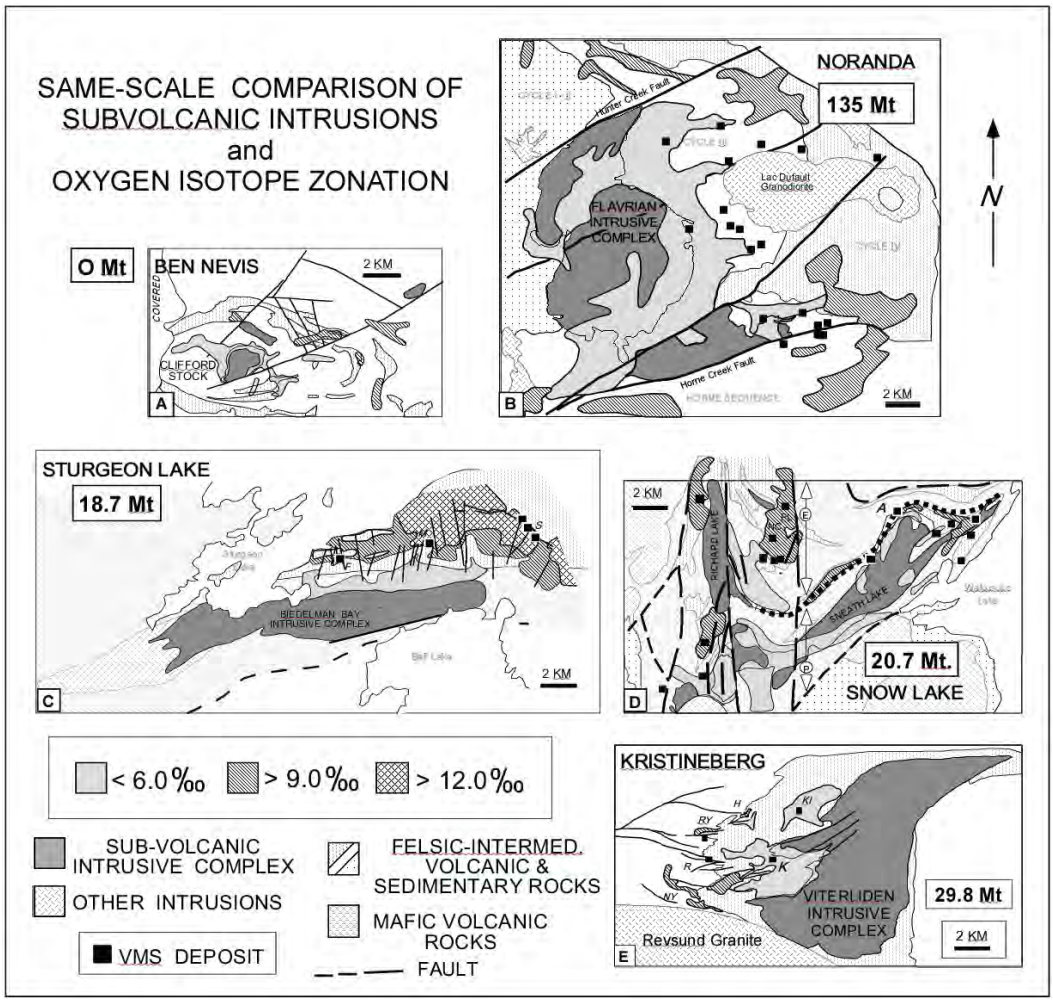

Fig. 3. The shapes of oxygen isotope zones associated with alteration about sub-volcanic intrusive complexes in a sub-marine environment reflect the local strain, yet still retain zoning systematics. Sizes of intrusions and high-temperature zones correlate approximately with total district tonnage of VMS

greenstone belt, Quebec. *Economic Geology*, **88**, 1483-1511.

CLAYTON, R.N. & MAYEDA, T. 1963. The use of bromine pentafluoride in the extraction of oxygen from oxides and silicates for isotopic analysis. *Geochimica et Cosmochimica Acta*, **27**, 43–52.

GALLEY, A. *et al.* 2002. Database for CAMIRO project 94E07: Inter-relationships between subvolvcanic intrusions, large-scale alteration zones and VMS deposits. *Geological Survey of Canada Open File* **4431.**

HOLK, G.J., TAYLOR, B.E., & GALLEY, A.G. 2008. Oxygen isotope mapping of the Archean Sturgeon Lake caldera complex and VMS-related hydrothermal system, Northwestern Ontario, Canada. *Mineral. Dep.*, **43**, 623-640.

MCNICOLL, V. *et al*. 2008. New U-Pb geochronology from the TGI-3 Abitibi/Plan Cuivre project: Implications for geological interpretations and base metal exploration. *Geological Association of Canada-Mineralogical Assocication of Canada Abstracts*, **33**, 110 p.

PIERCEY, S.J. *et al*. 2008. Syn-volcanic and Younger Plutonic Rocks from the Blake River Group: Implications for Regional Metallogenesis. *Economic Geology*, **103**, 1243-1268.

TAYLOR, B.E. 2004. Fluorination Methods in Stable Isotope Analysis. In: DEGROOT, P.A.(ed.), *Handbook of Stable Isotope Techniques,* **1**, Elsevier, Amsterdam, 400-472.

Exploration geochemistry, geochronology, and tracer isotopic data of copper mineralisation in dolomitic rocks, Dos Parecis Basin, Rondonia, Brazil

Aldo Vásquez[1,2], Pedro Perez[1], & Angelo Aguilar[1]
[1]*Codelco-Chile. Exploration Division, Huérfanos 1270, Santiago, CHILE.*
[2]*AMEC Internacional (Chile) S.A. Américo Vespucio 100, 2nd floor, Santiago CHILE*
(e-mail: aldo.vasquez@amec.com)

ABSTRACT: The Rondonia and Dos Parecis basins formed during the Neo-Proterozoic. Both are located in the south-western part of the Amazon Craton, Brazil. The Dos Parecis Basin is composed of two parallel sub-basins: Basin of Colorado in the north and Pimenta Bueno Basin in the south. A dolomitic layered unit crops out in the northern limit of the Colorado Basin and hosts copper sulphides, mainly chalcocite. The highest copper concentrations are found in white dolomites (4,137 ppm Cu on average), contained in primary chalcocite, and in copper and manganese oxides. The dolomitic unit has the highest concentrations of manganese (0.56% to 2.6% MnO). Surficial oxidation has produced anomalous concentrations of copper in soils (51 ppm to 98 ppm), and barium and manganese anomalies within 40 m to 160 m of the mineralised outcrops. The copper concentration in the fine fraction of stream sediments sampled from creeks cutting mineralisation varies downstream with anomalies not exceeding 135 ppm at 500 m to 1,000 m from the source.

Lead isotope ratios in chalcocite suggest a radiogenic lead contribution from the upper crust and give a Pb-Pb age of 800 Ma. In addition, chalcocite in dolomites has a high initial $^{87}Sr/^{86}Sr$ ratio, which is consistent with a high Rb/Sr ratio source typical of upper crustal rocks. The isotopic ratios in carbonates showed very low initial values of $^{87}Sr/^{86}Sr$ compared with the ratios for sea water from the Neo-Proterozoic to Permian; however, $^{87}Sr/^{86}Sr$ ratios of mineralised dolomitic carbonates have higher radiogenic isotope ratios than pure carbonates. There is a depletion of ^{13}C and ^{18}O in carbonates relative to normal sea carbonates, with values of $\delta^{13}C$ (PDB) between -5 and –4‰ and $\delta^{18}O$ (SMOW) between 23 and 25‰. The dolomites suffered a compositional change by reaction with an external source of fluid that affected their isotopic compositions as well as produced mineralisation.

KEYWORDS: *exploration, copper, isotopy, dolomites, Rondonia.*

INTRODUCTION

This work forms part of an effort to understand and to explore for the copper mineralisation discovered on the limits of the Dos Parecis Basin, Brasil. The mineralisation is associated with a unique dolomitic layer and corresponds to the presence of copper sulphides, mainly chalcocite. The study zone is located in the State of Rondonia, Brasil, 180 km to the south-east of the city of Ji-Parana.

This study sets forth the major conclusions resulting from geochemical exploration. Details of the complete exploration work are found in Aguilar *et al*. (2002).

GEOLOGICAL SETTING

Several large basins began to form during the Neo-Proterozoic on the Amazon Craton including the Rondonia Basin and Dos Parecis Basin. The Dos Parecis Basin is located on the southeast portion of the Amazon Craton, and is made up of magmatic and metamorphic rocks and by a Proterozoic to Cenozoic sedimentary and volcanic cover (Almeida *et al.* 1977).

REGIONAL GEOLOGY

The large sedimentary basins trend NW and contain extensive deposits. Sedimentation occurred from the Neo-Proterozoic to Mesozoic. The Dos Parecis Basin (Siqueira 1989; Pedreira & Bahía 2000) is comprised of marine and

continental volcanic deposits in two parallel sub-basins, one called the Colorado Basin in the south, and the other, the Pimenta Bueno Basin, in the north. Both basins are separated by paleo- to neoproterozoic rocks from the Guaporé Polycyclic Orogenic Belt. The oldest rocks of this belt comprise a large variety of orthogneiss and paragneiss, metavol-canic and metasedimentary rocks. Basic and acid igneous rocks, volcanic and intrusive, form also part of the youngest rocks of this belt (Scandolara 1999) (Figs. 1 and 2).

LOCAL GEOLOGY

The set of sedimentary rocks deposited in the Colorado Basin and the Cuenca Pimenta Bueno Basin during the Palaeozoic gave rise to the Dos Parecis Basin (Pinto Filho *et al*. 1977). The Colorado Basin shows the following stratified units: a) basal conglomerate; b) dolomitic unit (DU); c) sandstones, siltstones and micaceous lutites; and d) red micaceous feldspar sandstones. The DU contains three units: a sedimentary breccia, a white dolomitic unit, and a pink dolomitic layer. The white dolomitic layer is the unit containing copper suphide mineralisation, almost exclusively consisting of chalcocite, although covellite and digenite have also been identified. The carbonate rocks are correlated with the dolomitic layers in the Cacoal Formation of Palaeozoic defined by Siqueira (1989). The rocks of the Cacoal Formation are widely distributed in southern part of the Rondonia State and form part of the base of Dos Parecis Basin (Figs. 1 and 2).

The dolomitic rocks were affected by an alteration process evidenced by a bleaching of the rock at its base (Jones & Rehnfeldt 2001). The primary copper mineralisation is associated solely with the bleached portion of this dolomitic layer. Occasionally traces of copper oxides are observed in the basal conglomerate.

EXPLORATION GEOCHEMISTRY

Samples of rocks, core samples, stream sediments, panned semi-concentrate and soil samples were collected to study the supergene dispersion patterns related to the mineralisation on the surface. Other samples were collected for stable and radiogenic isotopic analysis to determine the ages of granitoid rocks and mafic dykes cropping out in the area, and to characterise the sources of mineralising fluids and their interaction with the host rocks.

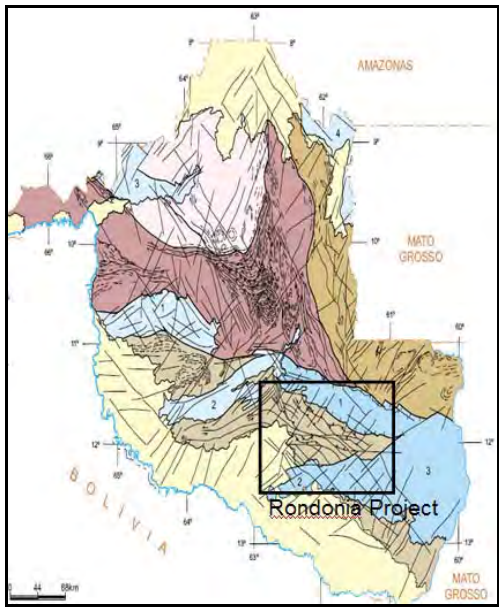

Fig. 1. Geology of the Rondonia State, Brazil.

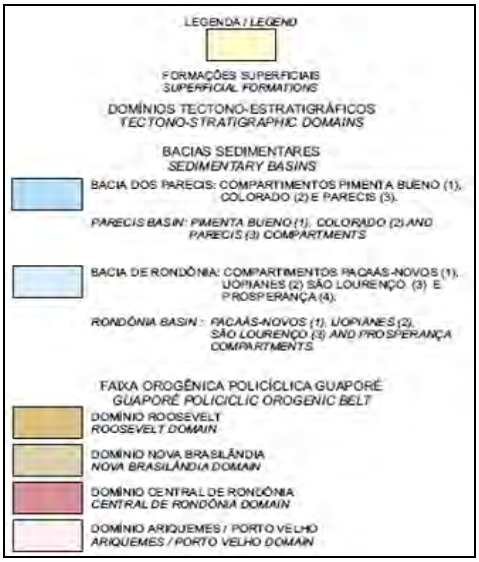

Fig. 2. Legend for map shown in figure 1.

Geochemical analyses were done at Geosol Laboratory in Belo Horizonte, Brazil and consist of multi-element determinations through plasma spectrometry (ICP-AES) and Au through fire assay on 30 g of sample or using aqua regia digestion and atomic absorption. The sample digestion was done with aqua regia, or through a multi-acid digestion with hydrofluoric acid. The geo-chronology and stable isotope analyses were performed at the University of Sao Paulo.

ROCK GEOCHEMISTRY

The highest copper concentrations are contained in white dolomites (4,137 ppm on average) where primary chalcocite and copper and manganese oxides occur. No concentrations of interest in Au, Ag, Pb and Zn were detected in the dolomites. The dolomitic unit shows the highest concentrations in Mn (0.56% to 2.6%).

The basal conglomerate unit shows high and variable copper concentrations (142 ppm to >5,000 ppm). The high concentrations are due to the presence of copper oxides in fractures filling spaces between clasts. Copper oxides are observed where white, mineralised dolomite overlies the conglomerate.

Basement rocks contain locally high copper concentrations (1,529 ppm maximum). This unit locally has copper sulphides and oxides. Mafic dykes and basement rocks do not show anomalous concentrations of Au, Ag, Cu, Pb, Zn or Mo.

SOIL GEOCHEMISTRY

Anomalous Cu concentrations in soil samples taken from the B horizon (60 cm to 90 cm) occurs between 40 m and 160 m from the mineralised outcrops with sample concentrations between 51 ppm and 98 ppm, and local maximum values up to 2,580 ppm along with barium and manganese anomalies.

STREAM SEDIMENT GEOCHEMISTRY

Samples of drainage sediments and pan concentrates of heavy minerals were collected. Chemical analysis was undertaken on the fine fraction (-270# and +400#), on the coarse fraction (-35# y +65#) of stream sediments and on whole-pan concentrates. Sediments in creeks cutting the non-mineralised sedimentary rocks contain copper concentrations between 7 ppm and 17 ppm in the coarse fraction; 21 ppm to 25 ppm in the fine fraction and variable concentrations between 34 ppm and 108 ppm in the whole-pan concentrates. Anomalous values for stream sediment samples containing detritus with copper oxides range from 51 ppm to 145 ppm in the fine fraction and 44 to 830 ppm in the pan concentrates. Copper concentration in the coarse fraction varies from 19 ppm to 39 ppm, up to anomalous values of 193 ppm and 290 ppm. The observed copper concentrations in the fine fraction, related to the distance downstream from the mineralised outcrops, is 39 ppm to 77 ppm between 0 and 500 m; 99 ppm to 135 ppm between 500 and 1000 m; 90 ppm between 1000 and 2500 m and less than 53 ppm at distances greater than 2500 m.

GEOCHRONOLOGY AND TRACER ISOTOPES

Lead, Sr, C and O isotope compositions were measured in carbonates of the dolomitic unit and in chalcocite concentrate. U-Pb and K-Ar radiometric dates were obtained from basement rocks and mafic dykes. The analysis were undertaken and The University of Sao Paulo under supervision of Professor C. Tassinari (Tassinari 2002).

GEOCHRONOLOGY

Maximum ages obtained from the basement rock samples correspond to a biotite and amphibole syenite (sample 1031) at 1,527.6 ± 4.5 My (U/Pb in zircons).

The basement rocks are cut by mafic dykes with epidote and biotite which showed the ages in Table 1.

The ages obtained for the basement rocks and mafic dykes show a maximum age that corresponds to the beginning of sedimentation at approximately 900 Ma.

Table 1. K/Ar ages in Mafic dykes.

Sample	Age (My)	Mineral
1019	1.042,7 ± 25,2	K-feldspar
1019	919,0 ± 16,2	whole rock
1030	955,5 ± 15,5	K-feldspar
1030	902,3 ± 16,4	whole rock

Table 2. Lead isotope ratios in chalcocite.

Sample	$^{206}Pb/^{204}Pb$	$^{207}Pb/^{204}Pb$	$^{208}Pb/^{204}Pb$
1026A	19,048	15,674	38,638
1026B	19,086	15,710	38,749
NB 18-13A	18,916	15,672	38,493
NB 18-13B	18,976	15,699	38,630

TRACER ISOTOPES

The lead isotope analyses of chalcocite concentrates gave the isotopic compositions shown in Figure 2.

The Pb isotope ratios are consistent with young mineralisation (less than 800 My), Neo-Proterozoic to Palaeozoic and are similar to lead isotope ratios of epigenetic mineralisation. This suggests a radiogenic lead contribution from the upper crust. The isotopic curves generated by the plumbo-tectonic model of Zartman and Doe (1980) show that the isotopic ratios are below 800 Ma and correspond to crustal values.

The Sr isotopes show high initial $^{87}Sr^{86}/Sr$ ratios in chalcocites, consistent with a high Rb/Sr ratio source. These high ratios are typical of upper crustal rocks. The isotopic ratios in carbonates showed very low initial $^{87}Sr/^{86}Sr$ values compared with ratios for sea water from the Neo-Proterozoic to Permian. Thus, fluid interaction affected the carbonates producing Rb and Sr remobilisation. Comparatively, the Sr isotope ratios of mineralised dolomitic-carbonates in the study area show higher radiogenic ratios than pure carbonates. It is likely that a fluid interacted with the carbonates leading to higher $^{87}Sr/^{87}Sr$ ratios.

The dolomites are depleted in ^{13}C and ^{18}O relative to normal marine carbonates, having values of $\delta^{13}C_{(PDB)}$ between -5 and - 4‰ and $\delta^{18}O_{(SMOW)}$ between 23 and 25‰. This could confirm a change of isotopic composition of carbonates produced by an external fluid.

CONCLUSIONS

The white dolomitic unit show high copper concentrations due to the presence of copper sulphides, consisting almost exclusively of chalcocite. No anomalous concentrations were found for Au, Ag, Pb, and Zn.

The basal conglomerate unit shows high and variable copper concentrations where secondary copper oxides formed as products of alteration of the overlying white dolomitic rocks.

(1) The copper concentration threshold for soil samples ranges from 54 ppm to 63 ppm.

(2) Expected copper concentrations in the fine fraction of stream sediments in creeks cutting mineralised outcrops do not exceed 135 ppm at 500 m to 1,000 m downstream.

(3) The lead isotope ratios indicate an upper crustal source for the lead and are consistent with mineralization at 800 Ma. Tracer isotopes in carbonates and chalcocite concentrates indicate that an external fluid altered the dolomitic unit changing its isotopic composition as well as deposited copper mineralisation.

ACKNOWLEDGEMENTS

We thank the Codelco Exploration Division for permitting this publication and allowing the comprehensive study, for which they provided fund and logistic support to carry out the exploration in this unrecognised and unexplored area of the planet. We thank the team for all discussions and conclusions.

REFERENCES

AGUILAR, A, FAUNDEZ, P., MENDEZ, A., PEREZ, P., VASQUEZ, A., & VIEGAS, E. 2002. Proyecto Rondonia. *Internal Publication, Codeco Chile*.

ALMEIDA F.F.M.; BRITO NEVES, B.B.; & FUCK, R.A. 1977. Porvincias estructurais brasileiras. In: *SBG, Simposio de Geologia do Nordeste*, **8**, Campina Grande, Atlas, 363-391.

JONES C.E. & REHNFELDT, J. 2001. Proyecto Nova Brasilandia, Rondonia Brasil, Resultados del Proceso de Due Diligence. *Internal Report Codelco Chile*.

PEDREIRA, A.J. & BAHIA R.B.C. 2000. Sedimentary Basins of Rondônia State, Brazil: Response to The Geotectonic Evolution of the Amazonic Craton. In: *Revista Brasileira de Geociências*.

PINTO FILHO, F.P.; FREITAS, A.F. DE; MELO, C.F. DE; ROMANINI, S.J. Projeto Sudeste de Rondonia. Relatorio Final. Porto Velho: CPRM, 1977. 4v.il. Convenio DNPM/CPRM.

SCANDOLARA, J. E. *et al.* 1999. Geologia e Recursos Minerais do Estado de Rondônia. *Texto Explicativo do Mapa Geológico do Estado de Rondônia*. CPRM.

SIQUEIRA, L.P. 1989. *Bacia dos Parecis. Boletim de Geociências da Petrobrás*.

TASSINARI, C. 2002. Relatorio Interpretativo dos dados isotopicos. Projecto Nova Brasilandia – Parecis. *Internal Report, Codelco*.

ZARTMAN, R.E. & DOE, B.R. 1981. Plumbotectonics, The Model. *Tectonophysics*.

The nature and significance of lithogeochemical and stable isotope alteration halos in the Hollinger-McIntyre gold deposit, Ontario, Canada.

Gibran D. Washington[1], Mona C. Sirbescu[2], Kevin T. Jensen[2], & Edmond H. van Hees[1]

[1]Wayne State University, Detroit, MI USA (midas@wayne.edu)
[2]Central Michigan University, Mt. Pleasant, MI USA

ABSTRACT: Two distinct mineralizing fluids formed the Hollinger-McIntyre-Coniaurum (HMC) deposit. The earliest fluid was associated with emplacement of a disseminated Cu-Au-Mo zone in the Pearl Lake Porphyry (PLP). The alteration pattern of the felsic rocks in the PLP is characterized by increased concentrations of K_2O, Au, Cu, Mo, W, and Sn, and K/Al, Sericite / Chlorite (SCI) and Sericite Alteration Indexes and the removal of CaO, relative to nearby "unaltered" rocks. The H_2O-CO_2-NaCl mineralizing fluid that altered the PLP had a temperature between 340° and 390°C, and a $\delta^{18}O_{water}$ composition of 11.7 to 12.7 ‰.

The H_2O-CH_4-CO_2-NaCl mineralizing fluid that deposited gold in and above the Hollinger Shear Zone (HSZ) had an estimated temperature of 290°C and a $\delta^{18}O_{water}$ of 4.6 ‰. This gold-bearing fluid was associated with increased concentrations of As, CO_2, and CO_2/CaO and removal of Na_2O from rocks in and above the HSZ. The isotopic composition of the auriferous fluid is similar to that of fluids that formed the Giant and Colomac deposits. Formation of the HMC Cu-Au-Mo and Au deposits by two geothermal systems with chemically distinct fluids has important implications for geochemical exploration efforts in the Porcupine Mining Camp and elsewhere.

KEYWORDS: *Hollinger, McIntyre, gold, mesothermal, lithogeochemical, alteration, stable isotope*

INTRODUCTION

Formation of mesothermal gold deposits is best studied in giant systems where geological conditions were optimal. The Hollinger-McIntyre-Coniaurum (HMC) is a giant deposit, located in the Porcupine Mining Camp of northeastern Ontario, that produced 891 metric tons of gold (31.4 million troy ounces) making it the largest mesothermal gold deposit in North America.

Two important, unanswered questions about mesothermal gold deposits include: (1) are they zoned chemically? and (2) was more than one mineralizing event involved in their formation? Studies of the Kolar gold field in India and the Sigma mine in Quebec found that gold fineness increased with depth. The occurrence of ankerite proximal to and calcite distal to gold veins in the HMC deposit has also been noted.

Studies of the Giant, Sigma, Dome, and Ptarmigan gold deposits found that they have complex fluid histories (van Hees *et al*. 1999; Gray & Hutchinson 2001; Shelton *et al*. 2004; Olivio *et al*. 2006; van Hees *et al*. 2006).

The lithogeochemistry of wall rocks in the Hollinger-McIntyre-Coniaurum (HMC) deposit has not been fully explored. The objective of this study was to characterize the lithogeochemical alteration of the wall rocks and the stable isotope geochemistry of the veins in order to: (1) test if the HMC deposit is zoned chemically; (2) determine how many mineralizing events were involved in forming the HMC deposit; and (3) identify fluid pathways involved in formation of the HMC gold deposit.

GEOLOGICAL SETTING

The HMC deposit occurs in the Archean-age Abitibi Greenstone Belt of northeastern Ontario, Canada. The deposit is hosted by the Tisdale assemblage of metavolcanic rocks that vary in composition from ultramafic at the

base (Hershey Lake Formation), to felsic at the top (Gold Center Formation) of the sequence. A number of younger felsic rocks, including the Pearl Lake Porphyry (PLP), have intruded these rocks. The east end of the PLP hosts Cu-Au-Mo mineralization that has been interpreted to be an Archean porphyry copper deposit formed at 2,672 ±10 Ma (Re/Os age), synchronous with the intrusion of late albitite dikes (Corfu *et al*. 1989; Ayer *et al*. 2003).

The Tisdale rocks were deformed by two tectonic events that resulted in superposition of east-west isoclinal folds on older north-south open folds. Five camp- to regional-scale faults, including the Hollinger Shear Zone (HSZ), have offset all these rocks. The HSZ is a reverse fault (~140 m offset) that passes through the Hollinger-McIntyre mine, strikes 57°, dips 65°S, extends to a depth of >1,500m and formed synchronous with the east-west folds. Most gold mineralization in the HMC deposit is associated with rocks in and above the HSZ.

The Abitibi greenstone belt has been metamorphosed to greenschist grade except where amphibolitic rocks are found adjacent to granite plutons and some gold deposits (Jolly 1978; Thompson 2005).

The HMC deposit has four alteration mineral assemblages that grade from the background greenschist facies to quartz-albite-ankerite-sericite proximal to individual veins (Smith & Kesler 1985). Studies of the HMC mine area have shown that higher concentrations of As, Ba, CO_2, Rb, K_2O, and As occur near gold-bearing zones (Whitehead *et al*. 1981). Specifically, either the CO_2/CaO molar ratio, or a combination of K_2O and As concentrations can be used to discern "mineralized" from "barren" zones.

Wall rocks in the HMC deposit have $\delta^{13}C$ values that range from -0.5 to -3.9 ‰ and $\delta^{18}O$ values that range from 9.7 to 14.2 ‰ (Kerrich & Hodder 1982). Quartz and carbonate in quartz-tourmaline-ankerite veins have $\delta^{18}O$ values that range from 10.6 to 17.6 ‰ and 11.4 to 14.3 ‰, respectively (Wood 1991).

ANALYTICAL METHODS

Rock samples collected from archived core, mine workings and outcrop were pulverized, homogenized, then analyzed using four-acid dissolution (SGS Lab, Toronto) to determine the near-total lithogeochemical composition (cassiterite, rutile, monazite, zircon, sphene, gahnite, chromite and barite are partially dissolved). Gold analyses were done by Fire Assay with Atomic Absorption finish on 30g samples and have a detection limit of 5 ppb.

The $\delta^{13}C$ and $\delta^{18}O$ analyses were performed on vein carbonate by the University of Waterloo stable isotope lab.

RESULTS AND DISCUSSION

Sericite/chlorite alteration index (SCI) and the CO_2/CaO molar ratios (Figs. 1 and 2, respectively) are plotted on north-south cross-sections through the HMC deposit. The highest abundance of sericite occurs in the felsic intrusive rocks such as the Pearl Lake Porphyry (Fig. 1), whereas the highest CO_2/CaO molar ratio occurs in and above the Hollinger Shear Zone (Fig. 2). These two geochemically distinct trends are mimicked by a number of the other elements. Addition of Au (Fig. 3) K_2O, Cu, Mo, W, and Sn, and the removal of CaO. High K/Al and Sericite Alteration Indexes have similar distributions as the SCI index, and follow the felsic rocks. The addition of As and CO_2, and the removal of Na_2O mimic the CO_2/CaO ratio by following rocks in and above the HSZ.

The association of the SCI alteration pattern with the Pearl Lake Porphyry and other felsic rocks is interpreted to indicate that they acted as a fluid conduit and permitted the vertical movement of the fluids through the fractured rocks in order to form the Cu-Au-Mo deposit.

The CO_2/CaO anomaly appears to indicate that Au deposits associated with the HSZ were formed by fluid that moved up along the HSZ, rather than by fluid moving through the felsic rocks.

The low $\delta^{18}O_{Cc}$ composition of vein carbonate in the PLP (Fig. 4) indicates that fluids reacted with the felsic wall rocks as they passed through them. The

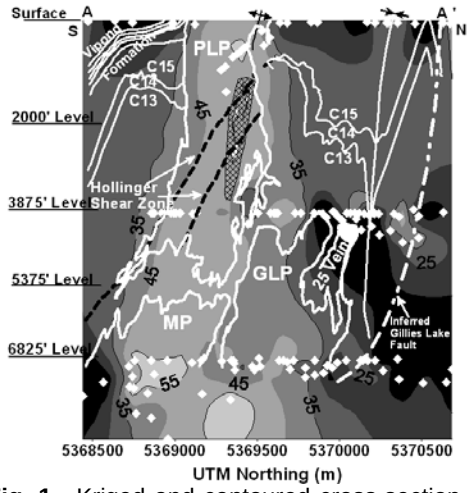

Fig. 1. Kriged and contoured cross-section of sericite / (sericite + chlorite))*100 Index (plotted in percent) along A - A' on McIntyre grid line 3500E through the HMC deposit. White diamonds indicate sample locations. Specific rock units such as C15 are labeled with abbreviations. The Cu-Au zone is indicated cross-hatching.

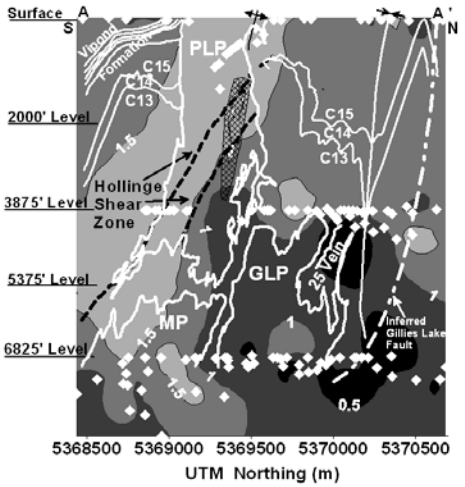

Fig. 2. Kriged cross-section of CO_2/CaO molar ratio along A - A' on McIntyre grid line 3500E through the HMC deposit has been modified by hand to reflect section geology. White dots indicate sample locations.

decrease in $\delta^{18}O_{Cc}$ from 14 to 12 ‰, as fluids moved up the HSZ, is also consistent with the mineralizing fluid reacting with the wall rock and implies a low water / rock ratio.

Coupling fluid inclusion temperature measurements with $\delta^{18}O_{Cc}$ values permits $\delta^{18}O_{water}$ of the mineralizing fluids to be determined. The McIntyre Cu-Au-Mo and Au fluids have distinctly different fluid compositions (Fig. 5), indicating that the mineralized zones were formed by two different hydrothermal systems. The compositions of the fluids that formed the HMC Au-bearing veins are comparable to those that deposited Au in the Giant and Colomac mines.

Failure to recognize that two distinct mineralizing fluids were involved in the formation of the HMC deposit resulted in at least two different alteration patterns being lumped together. Exploration carried

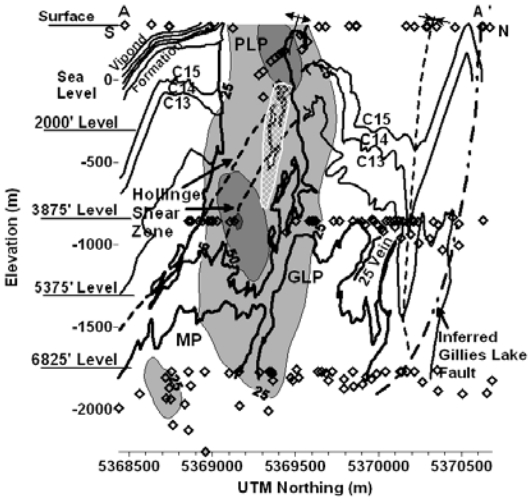

Fig. 3. Kriged and contoured cross-section of Au along A - A' on McIntyre grid line 3500E (white = 0-24 ppb, grey = 25-49 ppb, medium grey = 50-74 ppb, dark grey = 75+ ppb). Diamonds indicate sample locations.

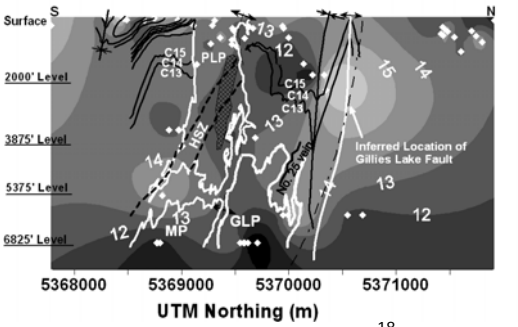

Fig. 4. Kriged cross-section of $\delta^{18}O_{Cc}$ along McIntyre grid line 3500E through the HMC deposit. White dots indicate sample locations.

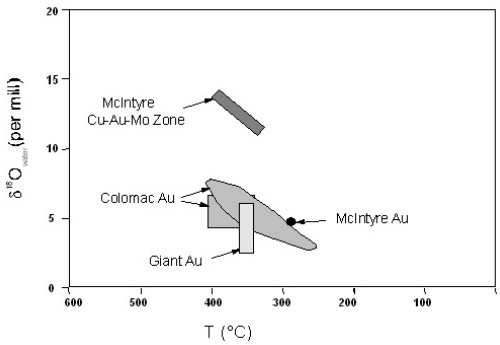

Fig. 5. Stable isotope composition of fluids that formed the Au and Cu-Au mineralization in the HMC mine. Comparative data is from the Giant and Colomac deposits (Shelton *et al*. 2004).

out using a single rather than two distinct geochemical models could be problematic.

SUMMARY

The results indicate:
(1) two chemically distinct fluids formed Cu-Au-Mo and Au mineralization in the HMC Deposit.
(2) Cu-Au-Mo and Au mineralizing fluids followed different hydrothermal conduits.
(3) Failure to recognize deposits that were formed by complex fluid histories could result in unique geochemical model with a low probability of success being used to exploration for new deposits.

ACKNOWLEDGEMENTS

We thank the former Pamour Porcupine Mines and Placer Dome Canada Ltd. for permission to sample and financial support. Drs. Larry Lemke and Carl Freeman helped plot and interpret the data. Stable isotope analyses were provided by Mr. Bob Drimmie at the University of Waterloo. Bruce Taylor is thanked for his review of an earlier version of the manuscript.

REFERENCES

AYER, J.A., BARR, E., BLEEKER, W.C. *et al.* 2003. New geochronological results from the Timmins area: Implications for the timing of late-tectonic stratigraphy, magmatism and gold mineralization. Ontario Geological Survey *Summary of Field Work 2003*, 33 p.

CORFU, F., KROUGH, T.E., KWOK, Y.Y., & JENSEN, L.S. 1989. U-Pb zircon geochronology in the southwestern Abitibi greenstone belt, Superior Province. *Canadian Journal Earth Sciences*, **26**, 1747-1763.

GRAY, M.D. & HUTCHINSON, R.W. 2001. New Evidence for Multiple Periods of Gold Emplacement in the Porcupine Mining District. *Economic Geology*, **96**, 453-476.

JOLLY, W.T. 1978. Metamorphic history of the Archean Abitibi Belt. *Geological Survey of Canada Paper,* **78-10**, 63-78.

KERRICH, R. & HODDER R.W. 1982. Archean Lode Gold and Base Metal Deposits: Evidence for Metal Separation into Independent Hydrothermal Systems, Geology of Canadian Gold Deposits: *Canadian Institute of Mining and Metallurgy*, 144-160.

OLIVO, G.R., CHANG, F., & KYSER, T.K. 2006. Formation of the auriferous and barren North Dipper veins in the Sigma Mine, Val d'Or, Canada; constraints from structural, mineralogical, fluid inclusion, and isotopic data. *Economic Geology*, **101**, 607-631.

SHELTON, K.L., MCMENAMY, T.A., VAN HEES, E.H., & FALCK, H. 2004. Deciphering the Complex Fluid History of a Greenstone-Hosted Gold Deposit: Fluid Inclusion and Stable Isotope Studies of the Giant Mine, Yellowknife, Northwest Territories, Canada. *Economic Geology*, **99**, 1643-1663.

SMITH, T.J. & KESLER, S.E. 1985. Relation of fluid inclusion geochemistry to wallrock alteration and lithological zonation at the Hollinger-McIntyre gold deposit, Timmins, Ontario. *Canadian Institute of Mining Bulletin*, **78**, 35-46.

THOMPSON, P.H. 2005. A New Metamorphic Framework for Gold *Exploration-Kirkland Lake Area, Western Abitibi Greenstone Belt: Discover Abitibi Initiative,* Open File Report **6205**, 104 p.

VAN HEES, E.H., SHELTON, K.L., MCMENAMY, T.A., ROSS, L.M. JR., COUSENS, B.L., FALCK, H., ROBB, M.E., & CANAM, T.W. 1999. Metasedimentary influence on metavolcanic-rock-hosted greenstone gold deposits: Geochemistry of the Giant mine, Yellowknife, Northwest Territories, Canada. *Geology*, **27**, 71-74.

VAN HEES, E.H., SIRBESCU M-L., WASHINGTON, G.D., BENDA, K.J., SHELTON, K.L., FALCK, H., & TRENAMAN, R.T. 2006. Genesis of the Ptarmigan Gold Deposit: is it of magmatic affinity?. In: A.D. ANGLIN, H. FALCK, D.F. WRIGHT & E.J. AMBROSE (eds.), *Gold in the Yellowknife Greenstone Belt, Northwest*

Territories, GAC-MDD Special Pub. No.3, 270-285

WHITEHEAD, R.E., DAVIES, J.F., CAMERON, R.A., & DUFF, D. 1981. Carbonate, alkali and arsenic anomalies associated with gold mineralization, Timmins Area. *Misc. Publication*, 318-333.

WOOD, P.C. 1991. The Hollinger-McIntyre gold-quartz vein system, Timmins, Ontario: Geological characteristics, fluid properties and light stable isotope geochemistry. *Ontario Geological Survey Open File Report* **5756**, 289 p.

Sponsors

Symposium bags sponsor

ACME Analytical Laboratories Ltd.

Platinum sponsors

SGS

Anglo American

Gold sponsors

AREVA

Newmont – The Gold Company

Barrick

TGI3 Canada

Geological Survey Commission Canada

Silver Standard

maxwell DATASHED

Actlabs

FREEWEST – Freewest Resources Canada Inc.

Silver sponsors

ODM – Exploring Heavy Minerals

Thermo Scientific

Innov-X Systems – Innovative XRF Technologies

APEGNB / AIGNB

OZ

xstrata zinc

Adex

Bronze sponsors

PotashCorp – Helping Nature Provide

International Association of Geochemistry – IAGC – Est. 1962

New Nouveau Brunswick – Natural Resources and Energy / Ressources naturelles et Énergie

Department of Geology – University of New Brunswick

IAG